U.PORTO

MESTRADO ONCOLOGIA

ESPECIALIDADE EM ONCOLOGIA LABORATORIAL

Investigating the functional relevance of FOXM1 isoforms and truncated forms in breast cancer cell tumorigenesis.

Komal Khalil

M

2022

Komal Khalil.Investigating the functional relevance of FOXM1 isoforms and truncated forms in breast cancer cell tumorigenesis.

M.ICBAS.2022

Investigating the functional relevance of FOXM1 isoforms and truncated forms in breast cancer cell tumorigenesis.

Komal Khalil

INSTITUTO DE CIÊNCIAS BIOMÉDICAS ABEL SALAZAR

Komal Khalil

Investigating the functional relevance of FOXM1 isoforms and truncated forms in breast cancer cell tumorigenesis

Dissertação de candidatura ao grau de **Mestre em Oncologia** – **Especialização em Oncologia Laboratorial** – submetida ao Instituto de Ciências Biomédicas Abel Salazar da Universidade do Porto

Orientador: **Doutora Florence Janody**

Investigador Principal

Cytoskeletal Regulation & Cancer
i3S-Instituto de Investigação e Inovação em Saúde – Universidade do Porto

Coorientador: **Doutora Elsa Logarinho**

Investigador Principal

Aging and Aneuploidy
i3S-Instituto de Investigação e Inovação em Saúde – Universidade do Porto

ACKNOWLEDGEMENTS:

This project would not have been possible without everyone who contributed to its development in some way. I, therefore, dedicate it to all of you.

Foremost, I would like to express my gratitude to my supervisor, Dr Florence Janody for her continuous support, encouragement, and patient guidance for the duration of my master's project.

Many thanks to Dr Elsa Logarinho, my co-supervisor, for always being available to help and for encouragement.

I would like to specially thank my fellow laboratory members, Lídia, Sandra, Carla, Camila and all the new girls who recently joined our lab. Note of appreciation goes to Lídia and Sandra for motivating me and offering help when in need. I would like to thank Alice, whom I had the privileged to work with on this project, she was a constant support. I would like to thank all the members of Aging and Aneuploidy group, especially Filipa, Ana Rita, Rita, and Carlos. I would like to thank Joana Macedo in particular, for always helping me and for her advice whenever needed.

I also must thank Professor Carmen, Director of the Master's in Oncology, the person I will always look up to. Thank you for always being there for me and for everyone else.

I would also like to extend a special thanks to my parents and siblings who initially inspired me to pursue this journey. Their love and confidence in me is what has always kept me motivated during this journey.

A special mention to all my close friends, people who are like a second family to me and my support-system. I would not be completing this step in my life if it was not for the constant motivational speeches given by my best friends, Miguel and Catarina, thank you for always having my back.

ABSTRACT

Aging is the main risk factor for cancer development, and several aging hallmarks have been linked to tumorigenesis. The transcription factor FOXM1 has long been considered as oncogenic, due to its role on cell proliferation and for being upregulated in human carcinomas, contributing to almost all cancer hallmarks. However, FOXM1 N-terminus non-transcriptional function was recently disclosed as tumour suppressive, which could disclose FOXM1 repression during aging as risk factor for age-associated cancer. Using the human mammary epithelial cell line with conditional activation of the Src proto-oncogene (MCF10A-ER-Src), which recapitulates molecular events taking place during basal-like breast cancer progression, we investigated for dynamic changes in the expression of FOXM1 isoforms. We found that MCF10A-ER-Src cells express FOXM1A, B and C isoforms, but both transcript and protein levels remained unchanged during Src activation. It was previously shown that during the first 12 hours of Src induction, pre-malignant cells transiently accumulate actomyosin stress fibres and undergo cell stiffening, which sustains cell proliferation through ERK activation. We found that Src activation does not stabilize FOXM1 by promoting actin filament accumulation, nor does it cleave FOXM1 through ERK activation, events previously reported in other cancer models. However, our preliminary observations suggested that Src activation induces the transient nuclear translocation of FOXM1 in pre-malignant MCF10A-ER-Src, which appears to be required to induce proliferative capacity as determined by siRNA-mediated depletion of FOXM1. Therefore, we propose a model through which Src potentiates FOXM1 transcriptional activity in pre-malignant cells through its translocation to the nucleus, which might occur through FOXM1 phosphorylation directly by Src or by ERK activation.

RESUMO

O envelhecimento é o principal fator de risco para o desenvolvimento do cancro, e vários *marcadores* do envelhecimento têm sido relacionados com a tumorigénese. Neste trabalho, pretendemos abordar o papel do fator de transcrição multifacetado FOXM1 no cancro da mama. Por se encontrar tipicamente sobre-expresso em carcinomas humano, o FOXM1 tem sido considerado oncogénico, contribuindo para a maioria dos *marcadores* de cancro. No entanto, a função não transcricional do N-terminal do FOXM1 foi recentemente revelada como supressora tumoral, o que poderá sugerir que a repressão do FOXM1 durante o envelhecimento será um fator de risco para o aparecimento de cancro. Para averiguar esta hipótese, utilizamos uma linha celular de células epiteliais mamárias humanas com ativação condicional do proto-oncogene Src (MCF10A-ER-Src). Esta linha recapitula eventos moleculares que ocorrem durante a progressão do cancro da mama do tipo basal, e permite investigámos alterações dinâmicas na expressão das isoformas do FOXM1. Descobrimos que as células MCF10A-ER-Src expressam as isoformas FOXM1A, B e C, mas tanto a transcrição como os níveis proteicos permaneceram inalterados durante a ativação de Src. Previamente foi demonstrado que durante as primeiras 12 horas da indução de Src, as células pré-malignas acumulam transitoriamente fibras de stress de actomiosina e sofrem alterações mecânicas na estrutura celular, o que sustenta a proliferação através da ativação de ERK. Verificámos que a ativação de Src não estabiliza o FOXM1 ao promover a acumulação de filamentos de actina, nem cliva o FOXM1 através da ativação ERK, eventos reportados anteriormente noutros modelos de cancro. Contudo, as nossas observações preliminares sugerirem que a ativação Src induz a translocação nuclear transitória do FOXM1 em MCF10A-ER-Src pré-malignas, que parece ser necessária para induzir a capacidade proliferativa, como foi determinado em células com a depleção de FOXM1. Portanto, propomos um modelo através do qual o Src potência a atividade transcricional do FOXM1 em células pré-malignas através da sua translocação para o núcleo. Isto pode ocorrer através da fosforilação do FOXM1 diretamente por Src ou por ativação ERK.

TABLE OF CONTENTS

FIGURE INDEX

TABLE INDEX

LIST OF ABBREVIATIONS

ABPs	Actin Binding Proteins
AJs	Adheren Junctions
BIC	Breast Invasive Carcinoma
BUC	Bladder Urothelial Carcinoma
CA	Colon Adenocarcinoma
CDH1	Cadherin 1
CGM	Complete Growth Medium
CHECK-2	Checkpoint kinase 2
CRP	C-Reactive Protein
CSHS	Charcoal Horse Stripped Serum
DBD	DNA-Binding Domain
DMEM	Dulbecco's Modified Eagle Media
DNAm	DNA methylation
EDTA	Ethylenediaminetetraacetic acid
EGF	Epidermal Growth Factor
EGTA	Ethylene Glycol-bis(β-aminoethyl ether)-N,N,N′,N′-Tetraacetic Acid
EMT	Epithelial-Mesenchymal Transition
ER	Estrogen Receptor
ERK	Extracellular-signal Regulated Kinase
EtOH	Ethanol
FACS	Fluorescence Activated Cell Sorting analysis
F-actin	Filamentous actin
FBS	Fetal Bovine Serum
FL	Full length
FOXM1	Forkhead Box M1 transcription factor
FSC-A	Forward Scatter Area
FSC-H	Forward Scatter Height
G-actin	Globular actin
HER2	Human Epidermal growth factor Receptor 2
HSF-1	Heat Shock Factor 1
IF	Immunofluorescence
IGF-1	Insulin like Growth Factor 1
IL	Interleukin
IRDye	Infrared fluorescent dye
LA	Lung Adenocarcinoma
LSC	Lung Squamous Carcinoma
MAPK	Mitogen-Activated Protein Kinase
MCP-1	Monocyte Chemoattractant Protein 1
NRD	N-terminal Repressor Domain
Opti-MEM	Reduced serum media
p120ctn	p120-catenin
PA	Prostate Adenocarcinoma
PALB2	Partner and Localizer of BRCA2
PBS	Dulbecco's Phosphate Buffered Saline
PR	Progesterone Receptor

PTEN	Phosphatase and Tensin homolog
RCM-1	Robesta Costa Memorial Drug 1
ROI	Region Of Interest
RT	Room temperature
Rt-qPCR	Real time quantitative PCR
SASP	Senescence Associated Secretory Phenotype
SD	Standard Deviation
SDS	Sodium Dodecyl Sulfate
siRNA	Small Interference RNA
SSC-A	Side Scatter Area
TAD	C-terminal Transactivation Domain
TAM	Tamoxifen
TF	Truncated Form
TIG1	Tazarotene-Induced Gene 1
TNBC	Triple Negative Breast Cancer
TNF	Tumour Necrosis Factor

CHAPTER I

INTRODUCTION

1. Cancer and Aging – Two intricately bounded biological processes

Over the last century, advances in healthcare and technology have boosted the average life expectancy. According to the World Health Organization, the proportion of the world's population over 60 years old will increase from 12% to 22% by 2050, totalling nearly 2 billion people (*World Health Statistics 2022*, n.d.). Cancer is frequently referred to as a disease of ageing. Individuals over 60 are more than twice as likely as younger patients to get invasive cancer, with a median diagnosis age of 65 and a median death age of 74 (Laconi et al., 2020). As a result, the number of elderly cancer patients is on rise, posing a huge health burden globally.

Cancer and aging may appear to be diametrically opposed processes, nonetheless, the two traits are intricately bound and share several hallmarks, which are briefly described below (Figure 1).

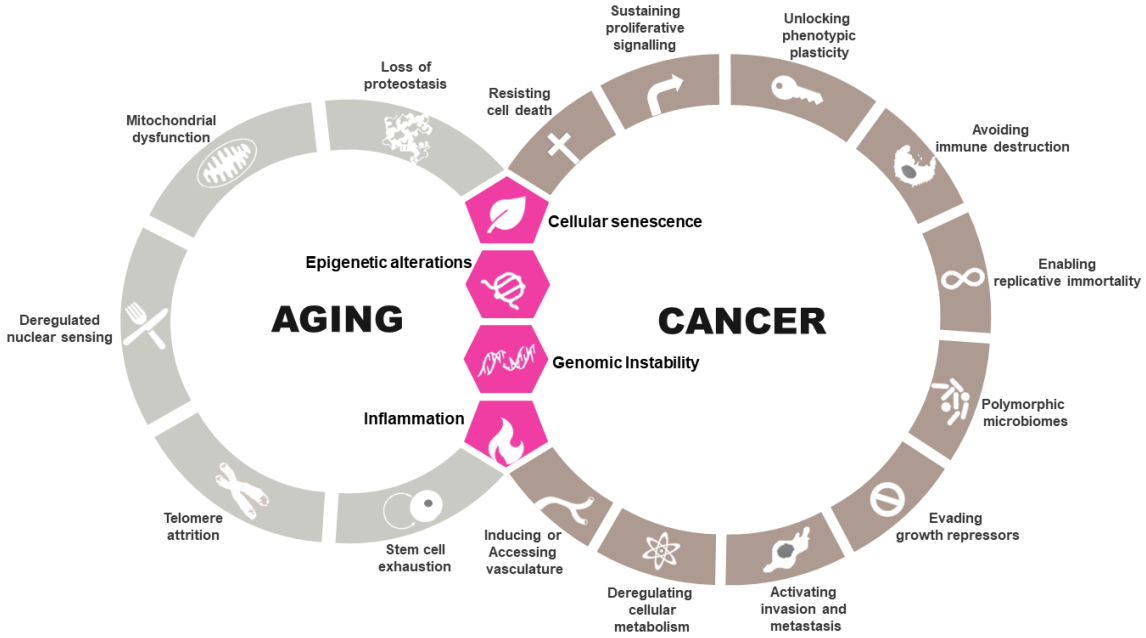

Figure 1. Schematic representation of shared and divergent hallmarks of Aging and Cancer. Cellular senescence, Epigenetic alterations, Genomic instability, and Tumour-promoting inflammation are four aging hallmarks proposed to contribute to the onset of cancer; categorized by López-Otín et al., 2013.

1.1. Cellular senescence

Cellular senescence is a permanent state of cell cycle arrest, triggered by various stress mechanisms such as telomere shortening, oncogene activation, DNA damage response pathway and activation of $p16^{INK4a}$ (Aunan et al., 2016). Senescence functions as an anticancer mechanism, by preventing the growth of damaged cells. Several possibilities may occur when a cell is damaged (Figure 2). Either can go into apoptosis or enter senescence as a result of activating an antiproliferative response. However, if it doesn't, the

cell can keep replicating and generate a tumour lesion and at this point, senescence and/or apoptotic processes may both be activated again. Eventually, these senescent cells keep on accumulating. Yet, if this is unsuccessful, the lesion might spread, cells may accumulate further genetic and/or epigenetic abnormalities, and finally a malignant tumour may arise. Even if cellular senescence is triggered, cells may still be able to circumvent it and undergo malignant transformation (due to epigenetic alterations, etc) (Berben et al., 2021). Thus, cellular senescence plays a role in maintaining tissue homeostasis by preventing the growth of damaged cells.

However, senescence can also have adverse effects. Senescent cells appear to accumulate with age, causing tissue to age and eventually failing organ homeostasis and function (Tchkonia et al., 2013; McHugh & Gil, 2017). Senescent cells can also potentially contribute to the development of tumours given that they are voracious secretors of pro-inflammatory cytokines, interleukins, and growth factors – a trait known as senescence associated secretory phenotype (SASP), which has been related to the onset of cancer and aging (Falandry et al., 2014).

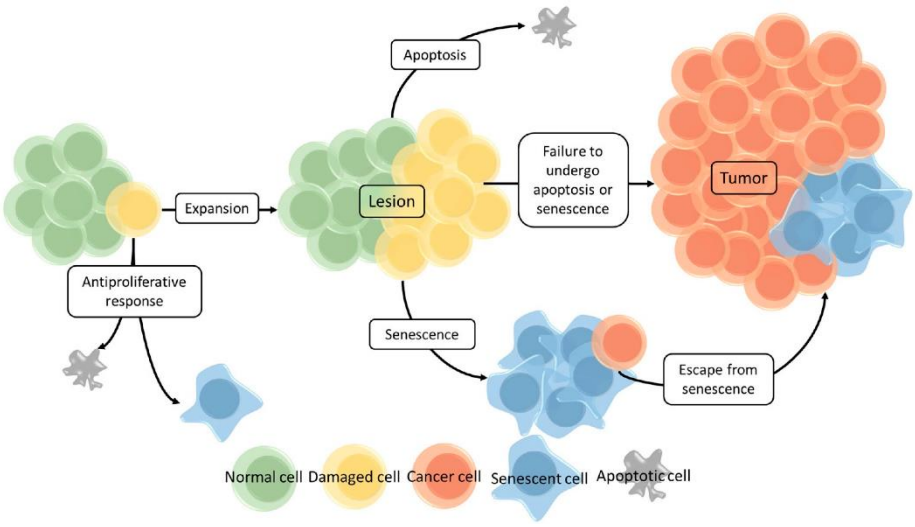

Figure 2. Schematic overview of cellular senescence role in promoting tumorigenesis. Possible outcomes of damaged cells include apoptosis or senescence (antiproliferative responses), and continued cell growth (expansion). When the latter happens, a lesion may develop where cells may once more go through the apoptotic or senescent processes. If adequate defensive systems are lacking or are ineffective, the lesion may grow further and, via the acquisition of new mutations, it can become a malignant lesion. In addition to this, senescent cells can also potentially break out of this state and develop into cancer cells. From Berben et al., 2021.

1.2. Genomic instability

Human body is susceptible to several mutagens, such as exogenous physical, chemical and biological agents, as well as by endogenous threats including DNA replication errors, spontaneous hydrolytic reactions, and reactive oxygen species (López-Otín et al., 2013).

These mutagens together cause loss of genomic integrity, cellular aging, and the onset of cancer (Vijg & Suh, 2013). Most tissues and organs usually experience a functional decrease as they age, although the precise pattern of these changes varies from person to person and is influenced by heredity and environmental factors. It is plausible that the degenerative phenotypes seen in aging individuals are more frequently caused by the accumulation of detrimental mutations that lead to senescence, apoptosis and eventually depletion of stem cells (Aunan et al., 2017; Maslov & Vijg, 2009). Therefore, genomic instability may be a major factor in aging, either directly or indirectly. Genomic instability also is a characteristic of almost all human cancers. And due to the accumulation of mutations, cancer cells can develop many of the features that make them more aggressive, including increased proliferation and metastatic potential (Hanahan & Weinberg, 2011).

A key player of the DNA damage response and one of the most important cellular gatekeepers is p53, a prime example of antagonistic pleiotropy. Low levels of p53 enable cells with tumorigenic mutations to proliferate and spread cancer, whereas high levels of p53 cause senescence and apoptosis that guard against damaging mutations and carcinogenesis (Maslov & Vijg, 2009; Zinger et al., 2017). Thus, genomic instability represents the deterioration of cells over time, resulting in programmed cell death and tissue loss with age. However, it also reflects the stochastic possibility of accumulating alterations that promote uncontrolled cell division and expansion in cancer, which can be supported by the increased lifetime cancer risk of tissues that require frequent cell cycles for homeostasis (Tomasetti & Vogelstein, 2015; Aunan et al., 2017).

1.3. Epigenetic alterations

Epigenetic alterations are modifications in gene expression without altering the DNA sequence, which includes non-coding DNA, histone modification, chromatin remodelling, and DNA methylation (Aunan et al., 2017). Many of the epigenetic alterations found in aging organisms have been linked to the progression and development of cancer, suggesting a possible association between age-dependent epigenetic changes and increased cancer risk in older individuals (Locke et al., 2019; Zhao & Shilatifard, 2019). The most well-known epigenetic alterations that links the aging epigenome and cancer are alterations in DNA methylation patterns (Figure 3). Global or localized DNA hypomethylation has been observed in a variety of tumour types, and intriguingly is also a major characteristic of aging cells (Witte et al., 2014). Additionally, carcinogenesis is thought to be aided by site-specific hypermethylation, which could suppress the expression of tumour suppressor genes. Age-dependent increases in the methylation of the promoters of several tumour suppressor genes, including LOX, p16/CDKN2A, and TIG1, have been observed in non-neoplastic gastric epithelia. This finding raises the possibility that a subpopulation of normal cells that

have already undergone methylation changes may be more susceptible to oncogenic transformation (So et al., 2006; Zabransky et al., 2022).

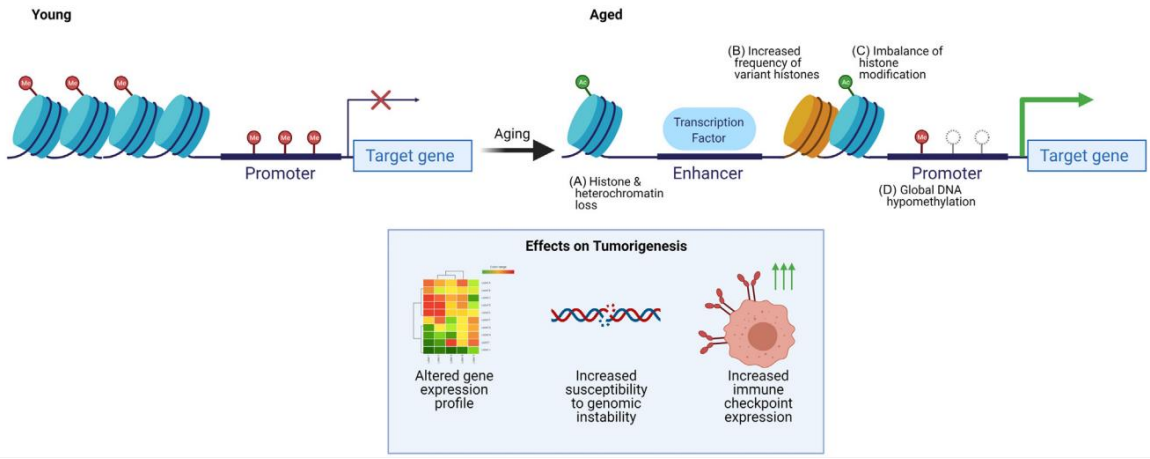

Figure 3. Age-related epigenetic alterations and their effects on tumorigenesis. (A–D) The epigenome can be altered by several ways during aging including (A) loss of histones and heterochromatin, (B) an increased frequency of noncanonical, variant histones, (C) imbalance in histone modifications, and (D) global DNA hypomethylation, among others. These modifications have been linked to tumour development and progression due to altered gene expression profile, genomic instability, and elevated expression of immunological checkpoint molecules in cancer cells (inset box). From Zabransky et al., 2022.

1.4. "Inflammaging" and Cancer

Inflammation is a complex biological response to harmful stimulus and its function is to eliminate the harmful agents, repair the damaged tissue and re-establish homeostasis. Inflammation can be acute or chronic. Acute inflammation is an overt rapid response to damage that is essentially beneficial and accelerates tissue repair. Chronic inflammation, on the other hand, is a low-grade sustained process that may eventually lead to tissue remodelling and dysfunction (Medzhitov, 2008; Zinger et al., 2017).

Aging has been associated with a low-grade, chronic state of inflammation, so-called inflammaging (Franceschi & Campisi, 2014). Chronic inflammation alters the microenvironment and the functioning of neighbouring cells; it interferes with anabolic signalling (e.g., by lowering IGF-1 levels via IL-6 and tumour necrosis factor alpha (TNF-)); and it impacts immunological responses. Numerous studies have shown that as people age, their levels of proinflammatory cytokines (such as IL-1, IL-6, and TNF-), chemokines (such as IL-8 and MCP-1), and other inflammation markers (such as CRP) gradually rise while their levels of anti-inflammatory mediators (such as IL-10) gradually decline. These inflammatory indicators are also linked to cellular senescence, more specifically the SASP, at the cellular level (Franceschi, 2007; Ostan et al., 2015).

Numerous evidence shows how multiple pathologic processes, including aging-related degenerative diseases and hyperplastic diseases like cancer, are aided in their initiation and/or progression by chronic inflammation (Vasto et al., 2007; Leonardi et al., 2018). Breast cancer serves as an example for the strong connection between pro-inflammatory environment and malignancy. In particular, it illustrates the link between IL-6, a key player in inflammaging, and the initiation and progression of cancer (Bonafè et al., 2012; Aunan et al., 2017). In individuals with breast cancer, high serum levels of IL-6 have also been associated with a poor prognosis (Knüpfer & Preiss, 2007).

2. FOXM1: A Multifaceted Transcription Factor

The transcription factor Forkhead Box M1 (FOXM1) is a strong candidate to reconcile the paradoxical aging-associated risk of carcinogenesis. Although FOXM1 is repressed during aging (Macedo et al., 2018), it is found typically upregulated in human cancers (Pilarsky et al., 2004). FOXM1, also known as HNF-3, HFH-11 or Trident, belongs to the superfamily of Forkhead Box (FOX) transcription factors (Korver, Roose, Heinen, et al., 1997). It is associated with several biological processes, including proliferation, cell cycle progression, cell differentiation, angiogenesis, apoptosis and DNA damage repair (Kalathil et al., 2021).

2.1. Regulation of FOXM1

The human FOXM1 gene is composed of 10 exons with two alternative exons referred as exons Va and VIIa, that are differentially spliced, giving rise at least four different isoforms with distinct localizations and functions: FOXM1A, B, C and D (Figure 4) (Korver, Roose, Heinen, et al., 1997; X. Zhang, Zhang, et al., 2017). FOXM1A contains both alternative exons, FOXM1B does not encompass any of the alternative exons, whereas FOXM1C retains only exon Va, and the newly discovered FOXM1D retains only exon VIIa. FOXM1A and FOXM1D are mostly found in the cytoplasm, whereas FOXM1B and FOXM1C are predominantly found in nucleus. The exon VIIa sequence in C-terminal of FOXM1A was demonstrated to suppress its transcriptional activity, and FOXM1B and FOXM1C have been reported to be transcriptionally active (Ngan et al., 2019; X. Zhang, Zhang, et al., 2017; Korver, Roose, Heinen, et al., 1997). All FOXM1 protein isoforms contain a conserved

forkhead DNA-binding domain (DBD), an N-terminal repressor domain (NRD), and a C-terminal transactivation domain (TAD) (Figure 4).

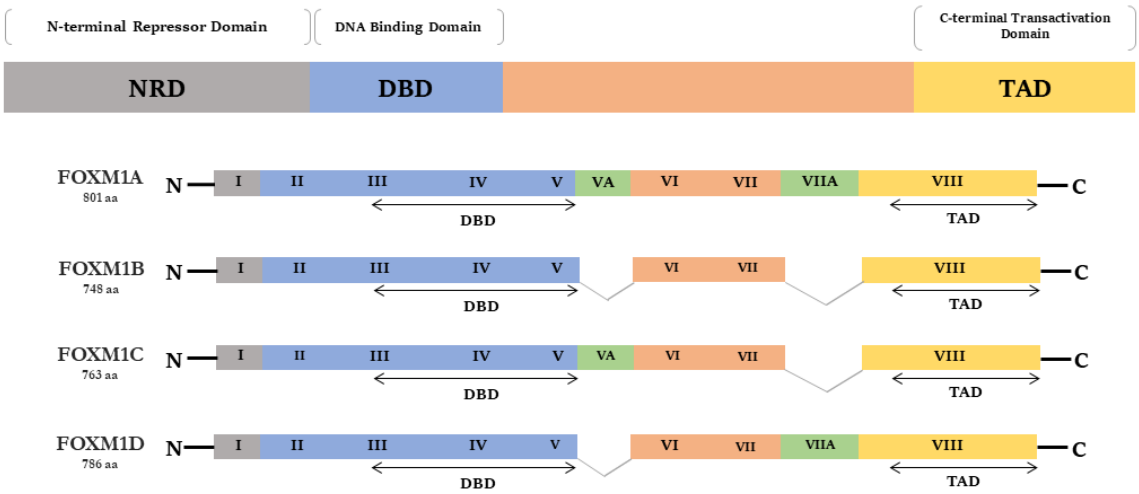

Figure 4. Schematic representation of the human FOXM1 gene and its isoforms. Human FOXM1 gene is composed of 10 exons (I–VIII), of which Va and VIIa (green) are alternatively spliced, giving rise to four FOXM1 isoforms – FOXM1A, FOXM1B, FOXM1C and FOXM1D. FOXM1 gene can be divided into three functional regions: a DNA-binding domain (DBD), an N-terminal repressor domain (NRD), and a C-terminal transactivation domain (TAD).

The FOXM1 gene has a specific expression pattern during the cell cycle and is undetectable in quiescent cells (Korver, Roose, & Clevers, 1997). As cells enter the S-phase of the cell cycle, FOXM1 expression rises, remains elevated during G2, and peaks during mitosis (Laoukili et al., 2007). Through the cell cycle, FOXM1's transcriptional activity increase is consistent with its phosphorylation status. During the G1 phase and at the beginning of the S-phase, FOXM1 proteins are relatively hypo-phosphorylated. The FOXM1 protein displays increasing phosphorylation from the S phase to the G2/M transition, achieves hyper-phosphorylation status in the M phase, and is then dephosphorylated in the late M phase. (Liao et al., 2018). This dynamic and tight phosphorylation and expression pattern is regulated by numerous cyclin-dependent kinases, that has been shown to relieve the autorepression of FOXM1 by the N-terminal inhibitory domain, restoring the TAD transcriptional activity (Kalathil et al., 2021; Anders et al., 2011). One of these kinases is the non-receptor tyrosine kinase c-Src, which activates FOXM1C by alleviating the inhibition of the TAD by its own auto-inhibitory N-terminus (Wierstra, 2011). It also has been discovered that FOXM1C has two Extracellular-signal Regulated Kinase (ERK) phosphorylation sites, at residues 331 and 704, and its phosphorylation by MAPK signalling promotes FOXM1C's nuclear translocation (Ma et al., 2005). Moreover, FOXM1C can undergo proteolytic processing upon stimulation of the ERK/MAPK signalling pathway (Lam et al., 2013). In addition to this, acetylation, SUMOylation, and ubiquitinoylation also contribute to the activity and stability of FOXM1 (Kalathil et al., 2021).

2.2. FOXM1 in Aging

FOXM1 expression positively correlates with cell/tissue proliferation rate. It is highly expressed in all embryonic tissues and in adult tissues with a high proliferation index (testes, thymus, and intestinal crypts) (Korver, Roose, & Clevers, 1997). Reduced expression of FOXM1 has been linked to mitotic abnormalities seen in cells from aged adults as well as from patients with progeria (a condition of rapid aging) (Ly et al., 2000). FOXM1 liver-specific deletion has been associated with a significant reduction in hepatocyte proliferation in adult mice following partial hepatectomy (X. Wang et al., 2001).

In FOXM1-depleted mouse embryonic fibroblasts, a transcriptional regulatory role of FOXM1 in cellular senescence was demonstrated (I.-C. Wang et al., 2005). Moreover, repression of FOXM1 in elderly cells was shown to induce genomic instability and trigger senescence, with typecast features including cytoskeletal changes and secretion of pro-inflammatory molecules (SASP) (Macedo et al., 2018). In addition, more recently, in progeroid and naturally aged mice, the *in vivo* cyclic induction of an active truncated form of FOXM1 (FOXM1-dNdK) was shown to increase the lifespan and improve aging-related phenotypes (Ribeiro et al., 2022).

2.3. FOXM1 in Cancer

FOXM1 ranks among the most significant genes identified as commonly upregulated in human carcinomas, including breast cancer (Abdeljaoued et al., 2017; Hamurcu et al., 2016) , ovarian cancer (Tassi et al., 2017), prostate cancer (Liu et al., 2017), colorectal cancer (H. Zhang et al., 2016), lung cancer (F.-F. Kong et al., 2014), gastric cancer (Okada et al., 2013), hepatoma (Egawa et al., 2017), angiosarcoma (Ito, Kohashi, Yamada, Iwasaki, et al., 2016) and melanoma (Ito, Kohashi, Yamada, Maekawa, et al., 2016). In fact, a dose-dependent correlation has been demonstrated between FOXM1 expression level and tumour progression, from cancer predisposition and initiation, to early pre-malignancy and progression, and finally to metastatic invasion (Teh, 2012; Wierstra & Alves, 2007) (Figure 5). However, FOXM1 has distinct N- and C-terminus functions that might account for FOXM1 two-edged sword role in age-associated tumorigenesis. Whereas its C-terminal transactivation domain sustains high proliferative capacity and other cancer hallmarks (Wierstra, 2013), its N-terminal domain acts antagonistically by preventing excessive cortical actin polymerization, chromosomal instability, and tumorigenesis (Limzerwala et al., 2020). Yet, the exact molecular mechanisms coupling the oncogenic vs. tumour suppressor functions of FOXM1 remain unknown.

It is evident that a wide range of FOXM1 functions, such as regulation of cell proliferation, DNA damage repair, inhibition of senescence and SASP are clearly associated with cellular aging, and consequently to the loss of organismal homeostasis. FOXM1 repression during cellular aging might act dually and antagonistically, with its proliferative function shutdown promoting senescence in damaged cells, and with SASP paracrine signalling and its non-proliferative function on cortical actin driving cellular transformation (Figure 5). Thus, FOXM1 appears an important molecular player to reconcile the paradoxical aging-associated risk for tumorigenesis.

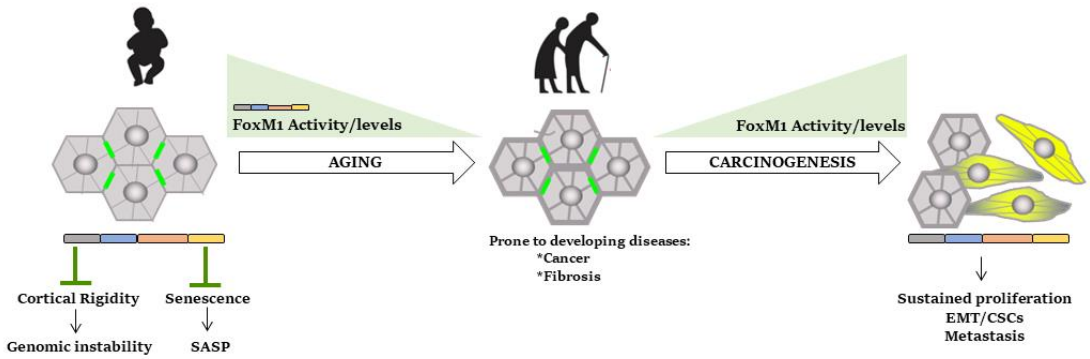

Figure 5. FOXM1 appears to be a key molecular player in reconciling Aging-Cancer Paradox. Repression of FOXM1 expression during aging can lead to genomic instability and trigger cellular senescence. Intriguingly, it ranks among the most significant genes identified as commonly upregulated in human carcinomas, contributing to all cancer hallmarks, including proliferation, epithelial-mesenchymal transition (EMT) and stemness.

3. The actin cytoskeleton

FOXM1 activity is tightly associated with actin cytoskeleton dynamics. Actin is a highly conserved intracellular cytoskeletal protein. It exists in two forms – monomeric, globular actin (G-actin), which polymerizes into filamentous actin (F-actin). F-actin is a major component of the cytoskeleton that regulates a variety of cellular functions such as cell division, differentiation, shape, polarity maintenance, contractility, mechanosensing and migration. The capacity of actin filaments to contribute to this vast range of functions results from their ability to organize into distinct populations with specific physical properties, controlled by the activity of actin binding proteins (ABPs) (Yogurtcu et al., 2013; Bajpai et al., 2021).

3.1. Actin cytoskeleton and Aging

A slew of studies has linked cellular/organismal aging and age-related diseases, ranging from cancer to neurodegeneration to disruption in the actin cytoskeleton's structure and dynamics (Khalil et al., 2022; Bajpai et al., 2021; Lai & Wong, 2020). Experiments in rats have shown a reduction in β-actin levels by 23% and 37% in 12 and 24-month-old animals

respectively, when compared with 6-month-old rats (Moshier et al., 1993). In *Drosophila*, a striking decrease in *act 79B* and *act 88* transcripts was observed during the first few days of adult life, down to a level of 10% or less in old flies (Labuhn & Brack, 1997). Furthermore, aged cardiac fibroblasts were described to exhibit reduced levels of the LOX-1 receptor that were associated with significant changes in morphology and proliferative capacity (X. Wang et al., 2013). In *Caenorhabditis elegans*, the structure and morphology of the actin cytoskeleton in the muscle, intestine, and hypodermis was shown to deteriorate with age. Interestingly, it has been discovered that modulating the expression of heat shock factor (HSF-1), a nodal protein implicated in several pathways of the heat shock response, has a direct impact on cytoskeletal regulation throughout aging. HSF-1 overexpression can help preserve cytoskeletal integrity during aging, but knocking it down causes the actin cytoskeleton to age prematurely (Higuchi-Sanabria et al., 2018).

Preserving the cytoskeletal integrity can have a beneficial impact on cellular and/or organismal lifespan. In yeast, the actin cytoskeleton was found to extend the lifespan by modulating mitochondrial inheritance. Actin cables, which are bundles of actin filaments that facilitate cargo transport in budding yeast, form a retrograde flow from the bud towards the mother cell. Actin flow is driven by actin polymerization and myosin-activity within the cell. This flow forces mitochondria to “swim upstream” and ensures that only healthy mitochondria reach the new cell, consequently extending its lifespan and health span (Higuchi et al., 2013; Higuchi-Sanabria et al., 2016). Furthermore, Kaushik and his colleagues examined vinculin-mediated cytoskeletal remodelling in *Drosophila* and showed that this mechanism delays aging by improving heart performance and extending organismal longevity (Kaushik et al., 2015).

3.2. Role of actin cytoskeleton in cancer

Given the role of the actin cytoskeleton in cellular activities like cell migration and division, it's easy to understand how its dysregulation might result in cancer (Izdebska et al., 2020). The actin cytoskeleton controls the activity of several signalling pathways, including Ras-MAPK, NF-kB, P13K, and the Hippo signalling pathways (Kustermans et al., 2008; Moujaber & Stochaj, 2020). It has been shown that pre-malignant cells accumulate polarized F-actin stress fibres, inducing a transient increase in cell stiffening. In turn, cell stiffening triggers the activation of ERK, which upregulates Cyclin D1 to sustain cell proliferation (Tavares et al., 2017). Moreover, recently it has been shown that the transient accumulation of F-actin in pre-malignant cells can trigger the MRTF-A/SRF signalling pathway, which in turn promotes the malignant transformation (Faria et al., 2022). It has also been demonstrated that actin dysregulation in human mammary cells activates the Wnt signalling pathway, encouraging cell proliferation and EMT (X. Zhang, Pei, et al., 2017).

Growing data suggests the FOXM1 and the actin cytoskeleton crosstalk in human cancer (Figure 6). In glioblastoma, FOXM1 protein stability is regulated by advillin through its role on F-actin dynamics, where FOXM1 induces an inflammatory microenvironment through LIN28B expression (Xie et al., 2020). Conversely, FOXM1D induces F-actin assembly by directly binding to ROCK2, promoting EMT and metastasis of colorectal cancer cells (X. Zhang, Zhang, et al., 2017). In addition, the N-terminal domain of FOXM1 prevents excessive cortical actin polymerization, which leads to chromosomal instability and tumorigenesis (Limzerwala et al., 2020). FOXM1 also affects the expression of ABPs (Vaz et al., 2021).

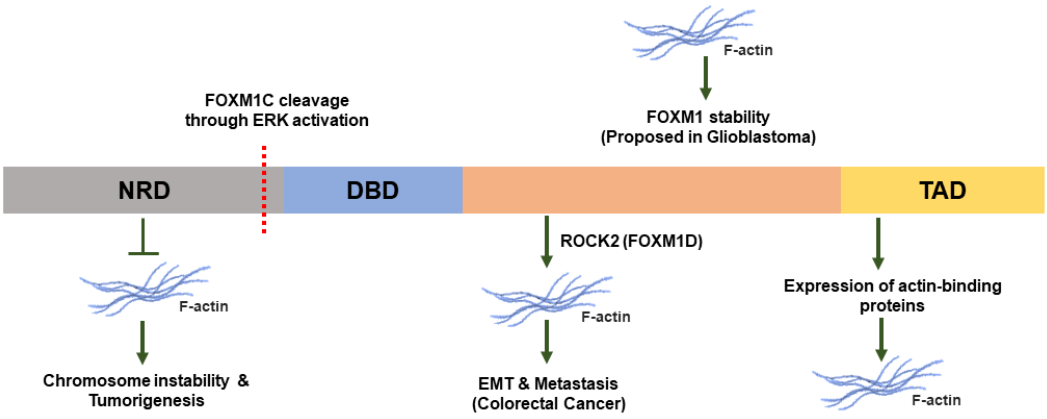

Figure 6. Schematic representation of FOXM1 and its crosstalk with F-actin. NRD represents N-terminal repressor domain, DBD represents DNA-binding domain and TAD represents C-terminal transactivation domain of FOXM1 protein.

4. Breast Cancer

4.1. Aging of Breast tissue

Emerging evidence suggests that breast tissue may age faster than the other tissues. As an epigenetic biomarker for biological aging, the DNA methylation (DNAm) clock has received widespread acceptance (Field et al., 2018). Breast tissue from healthy women were demonstrated to be epigenetically older when compared to blood (Sehl et al., 2017). The DNA methylation clock has been observed to accelerate significantly as a result of steroid receptor mutations in breast cancer (Panjarian et al., 2021; Horvath, 2013). Furthermore, breast tumour tissue was shown to have much greater epigenetic age acceleration than normal or adjacent-normal tissue, whereas there was no discernible difference between normal and adjacent-normal breast tissue. Breast cancer epigenetic clock acceleration appears to be related to certain clinical characteristics of the tumour, such as molecular subtype, grade, and stage. Significant DNAm age acceleration was observed in both the HER2+ and hormone-receptor positive subtypes. In contrast, in

aggressive molecular subtypes, such as triple-negative breast cancers (TNBCs) epigenetic age acceleration is reduced (Castle et al., 2020).

4.2. Epidemiology, Risk factors and progression

Breast cancer was and remains one of the most prevalent types of cancer among women. With recorded 2.3 million cases, breast cancer is the leading cause of cancer mortality worldwide among women (Sung et al., 2021) and global cancer incidence in 2020, surpassing lung cancer.

The correlation of epidemiologic and population studies conducted to date have established a variety of risk factors for breast cancer. The risk of developing breast cancer increases with age, early menarche, late menopause, late first full-term pregnancy, use of oral contraceptives and hormone replacement therapy. Diet, obesity, smoking, and alcohol use also increase the risk of breast cancer (Fahad Ullah, 2019). Another intrinsic factor conditioning the occurrence of breast cancer is the familial susceptibility. BRCA mutation carriers and mutations of other genes that are significantly involved in the neoplastic transformation such as CHEK2 (checkpoint kinase 2), PTEN (phosphatase and tensin homolog), PALB2 (partner and localizer of BRCA2), RAD51C, CDH1 (cadherin 1) or genes determining Lynch syndrome, confer increased risk to breast cancer (Y.-S. Sun et al., 2017; Kamińska et al., 2015).

Breast cancer arises in the lining of epithelial cells, which progresses to flat epithelial atypia (FEA), and then develops into atypical ductal hyperplasia (ADH), resulting in a ductal carcinoma *in situ* (DCIS) or invasive ductal carcinoma (IDC). *In situ* or pre-invasive carcinoma is a type of cancer that has not yet spread to the basal membrane and does not have the capacity to invade other organs. It grows inside of pre-existing normal lobules or ducts, but it can progress to invasive cancer. In invasive carcinomas, cancer cells infiltrate outside of the normal breast lobules and ducts and grow into the breast connective tissue. Invasive carcinomas have the potential to metastasize to other parts of the body, such as lymph nodes (Malhotra et al., 2010).

4.3. Molecular classification of Breast Cancer

Breast cancer is a highly heterogeneous disease and can be molecularly divided into different subtypes. The absence and presence of some receptors, such as estrogen receptor (ER), progesterone receptor (PR), human epidermal growth factor receptor 2 (HER2/neu) and Ki67 proliferation index are used to create a molecular classification that has been shown to have considerable prognostic and predictive significance for breast cancer. According to molecular classification, there are four distinct groups: Luminal A, Luminal B, HER2-enriched, and TNBCs (Table 1) (Johnson et al., 2021).

Table 1. Molecular subtyping of breast cancer. ER – Estrogen receptor; PR – Progesterone receptor; HER2 - Human epidermal growth factor receptor 2. Adapted from Johnson et al., 2021.

	ER	PR	HER2	Ki67	Prognosis
Luminal A	**+**	≥20%	**-**	<14%	Good
Luminal B	**+**	<20%	**-/+**	≥14%	Poor
HER2 enriched	**-**	**-**	**+**	Any	Poor
Triple negative	**-**	**-**	**-**	Any	Poor

As mentioned earlier, acceleration of epigenetic aging was not observed in TNBCs (Castle et al., 2020). Moreover, FOXM1 expression has been found to be increased in triple-negative breast cancers in comparison with the other breast cancer subtypes (Tan et al., 2019). Triple-negative breast cancers, which accounts for 15-20% of incident breast cancers, grow, and spread more quickly than the other subtypes of breast cancer (Johnson et al., 2021; Provenzano et al., 2018). Approximately 70% of triple-negative breast cancers are basal-like breast tumours and their gene expression overlaps by 56%. Both the basal-like and triple-negative phenotypes are connected to ductal carcinomas that are typically aggressive and highly invasive. TNBCs have the worse prognosis among breast cancer subtypes and has limited treatment options (Yin et al., 2020).

4.4. Inducible MCF10A-ER-Src cell line model

Using a human mammary epithelial cell line with conditional activation of the Src proto-oncogene (MCF10A-ER-Src), which recapitulates molecular events taking place during basal-like breast cancer progression, preliminary data in the lab suggested FOXM1 to be dynamically regulated during cellular transformation. This untransformed cell line contains a fusion between v-Src, the viral homologue of the human c-Src, and the ligand-binding domain of the estrogen receptor (ER), inducible with Tamoxifen (TAM) treatment (Hirsch et al., 2009; Iliopoulos et al., 2009). Previously, the lab reported that during the first 12 hours of Src induction, pre-malignant cells transiently accumulate actomyosin stress fibres and undergo cell stiffening, which sustain cell proliferation through ERK activation. In addition, stress-fibre-mediated cell stiffening further potentiates Src activation and is absolutely required for pre-malignant cells to suffer EMT 24 hours after TAM treatment. Moreover, these cells acquire cancer stem-like cell features 24 hours after TAM treatment and migrating abilities after 36 hours of Src activation (Figure 7) (Faria et al., 2022; Selvaggio et al., 2020; Jain et al., 2019; Tavares et al., 2017; Iliopoulos et al., 2009).

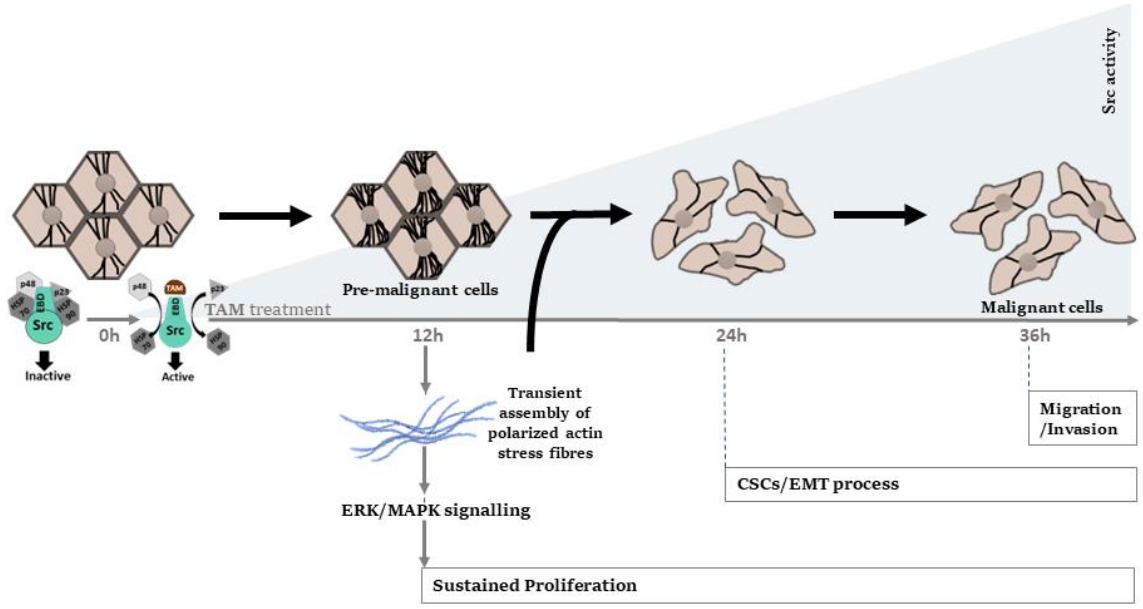

Figure 7. Schematic depicting the multistep acquisition of pre-malignant and malignant features in TAM-treated MCF10A-ER-Src cells. TAM induces Src activation resulting in a full transformation within 36 hours, which is not the case when cells are treated with the vehicle EtOH. During the first 12 hours of TAM treatment (pre-malignant cells), Src induces the transient assembly of polarized actin stress fibres which activates the ERK/MAPK signalling to sustain cell proliferation and promote malignant transformation. After 24 hours of TAM treatment, cells undergo EMT and acquire CSC characteristics. Later, after 36 hours of TAM treatment, they acquire migrating and invading abilities.

This temporary effect on the actin cytoskeleton could be associated with the transient accumulation of specific FOXM1 isoforms. Accordingly, preliminary observations suggested that FOXM1 accumulates in the nucleus and cytoplasm of pre-malignant MCF10A-ER-Src cells (Figure 8). Thus, the inducible MCF10A-ER-Src cell model offers the advantage to address the role of distinct FOXM1 isoforms and/or their truncated forms and how they are re-activated during the early stages of breast carcinogenesis.

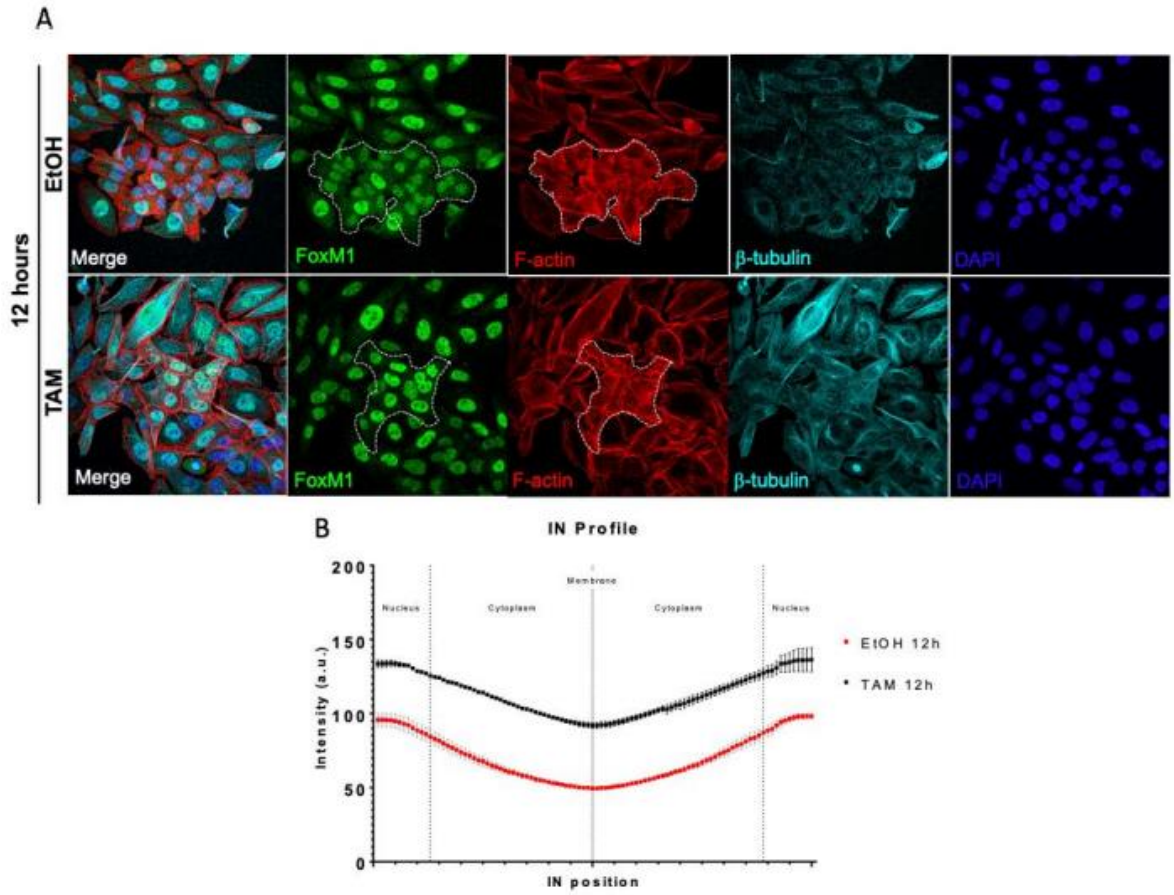

Figure 8. FOXM1 accumulates in the nucleus and in the cytoplasm in MCF10-ER-Src cells treated with TAM. (A) Standard confocal sections of MCF10A-ER-Src cells treated with EtOH or TAM for 12 h, stained with anti-FOXM1 (green), phalloidin (red) that stains F-actin, ß-tubulin (cyan) that stains microtubules and DAPI (blue) that stains the nuclei. The punctuated white dot lines delimit confluent cells that form AJs. (B) FOXM1 quantification in G1 cells with AJs (epithelial-like) in two biological replicates, using a program developed by Figueiredo et al.,2018.

CHAPTER II

PROJECT RATIONALE

This Master project was developed in the Cytoskeletal Regulation & Cancer group and in the Ageing and Aneuploidy group at i3S-Instituto de Investigação e Inovação em Saúde.

FOXM1 expression is repressed during aging (Macedo et al., 2018), however it is largely known to be overexpressed in many human carcinomas contributing to almost all cancer hallmarks (Kalathil et al., 2021). Previously, the Janody's and Logarinho's labs gathered preliminary data suggesting that FOXM1 could transiently accumulate in pre-malignant MCF10A-ER-Src cells (Figure 8). FOXM1 comes in different flavours (Gartel, 2017). However, it is unclear whether specific FOXM1 forms are oncogenic and whether they are required in pre-malignant cells for cellular transformation. To tackle these questions, we used the inducible MCF10A-ER-Src cell line, which recapitulates molecular events taking place during the transition from an untransformed state to a malignant phenotype (Tavares et al., 2017). Oncogenic forms of FOXM1 could accumulate in pre-malignant cells through three main mechanisms:

1st hypothesis: The FOXM1B and FOXM1C spliced variants have been demonstrated to have transforming ability (Huang et al., 2014; Lam et al., 2013). In addition, FOXM1D has been shown to promote EMT and metastasis in colorectal cancer cells (X. Zhang, Zhang, et al., 2017). Therefore, specific FOXM1 isoforms with oncogenic function could be upregulated in pre-malignant cells (Figure 9).

2nd hypothesis: FOXM1 stabilization by F-actin is required to promote tumorigenicity in glioblastoma (Xie et al., 2020). As pre-malignant MCF10A-ER-Src cells transiently accumulate F-actin (Tavares et al., 2017), F-actin-dependent stabilization of FOXM1 in pre-malignant cells could account oncogenic activity (Figure 9).

3rd hypothesis: ERK has been shown to cleave the FOXM1C isoform. FOXM1C cleavage could generate an oncogenic transcriptionally active form of FOXM1C lacking the N-terminal domain (Lam et al., 2013). In contrast, the FOXM1 N-terminal domain has been demonstrated to reduce cortical rigidity (Limzerwala et al., 2020). As the transient accumulation of F-actin in pre-malignant MCF10A-ER-Src cells is required to sustain cell proliferation through ERK activation (Tavares et al., 2017), ERK-dependent cleavage of FOXM1C could promote the acquisition of pre-malignant features, including proliferation or an inflammatory microenvironment, through the TAD domain, while accumulation of the FOXM1C N-terminal domain could provide a negative feedback, which reduces cortical rigidity, promotes F-actin disassembly and the acquisition of malignant phenotypes, including EMT (Figure 9).

To distinguish between these hypotheses, we asked three main questions:

1. **Does pre-malignant MCF10A-ER-Src cells upregulate one specific FOXM1 isoform?**

We first identified the FOXM1 isoforms that are upregulated in human carcinomas through *in silico* analysis using ISOexpresso database. We then performed quantitative real time PCR analysis using FOXM1 isoform-specific primers (X. Zhang, Zhang, et al., 2017) to determine if the expression of specific FOXM1 isoforms was altered in pre-malignant MCF10A-ER-Src cells compared to untransformed cells.

2. **Is FOXM1 stabilized or cleaved in pre-malignant MCF10A-ER-Src cells?**

We analysed FOXM1 levels, processing, and localization in pre-malignant MCF10A-ER-Src cells by western blot and immunohistochemistry using FOXM1 antibodies, which recognize all FOXM1 isoforms.

3. **Is FOXM1 required to sustain the proliferation of TAM-treated MCF10A-ER-Src cells?**

We analysed the effect of small interfering RNA depletion of FOXM1 (siFOXM1), that knocks down all FOXM1 isoforms or FOXM1A and FOXM1C, on the ability of pre-malignant MCF10A-ER-Src cells to sustain proliferation in the absence of Epidermal Growth Factor and low concentration serum.

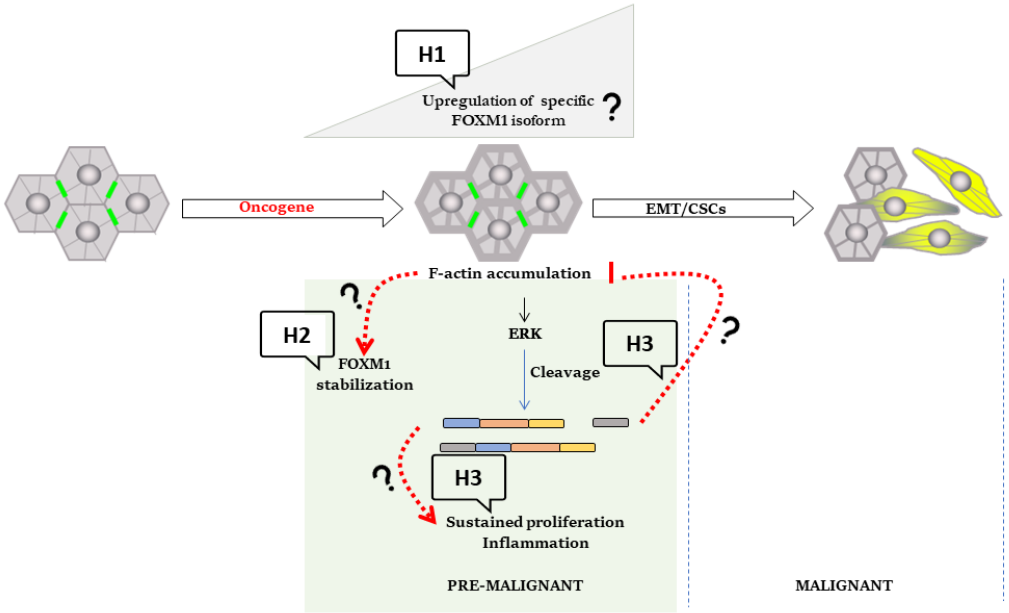

Figure 9. Model by which oncogenic form of FOXM1 could be induced in pre-malignant cells. Specific FOXM1 isoform could be upregulated in pre-malignant cells (H1- Hypothesis 1). Or FOXM1 could be stabilized through the F-actin accumulation (H2- Hypothesis 2) or could undergo proteolytic processing upon ERK activation in pre-malignant cells (H3- Hypothesis 3).

CHAPTER III

MATERIAL AND METHODS

1. MCF10A-ER-Src cell line culture conditions

The MCF10A-ER-Src cell line was kindly provided by Kevin Struhl (Hirsch et al., 2009). Cells were cultured in a *humidified incubator* set at 37°C with *5% CO_2* atmosphere, in Complete Growth Media (CGM), composed of DMEM/F12 growth media (Gibco™, 11039-047), supplemented with 5% of Charcoal Stripped Horse Serum (CSHS), 20 ng/mL human Epidermal Growth Factor (EGF) (Peprotech, AF-100-15), 0.5 µg/mL Hydrocortisone (Sigma, H0888), 100 ng/mL Cholera toxin from Vibrio cholerae (Sigma, C8052), 10 µg/mL Insulin (Sigma, I9278) and 0.5 µg/mL Puromycin (Merck, 540411).

1.1. Cell seeding protocol

Once the cells were 70% confluent in the flasks, culture media was aspirated and discarded. Cells were washed with sterile Dulbecco's Phosphate Buffered Saline (PBS1x) (Biowest, L0615) and trypsinized using TrypLETM Express (Gibco™, 12604-021) for 15 min in a *humidified incubator* set at 37°C with *5% CO_2* atmosphere. To inactivate the trypsin, 2 volumes of CGM were added to the flask and the cell suspension was transferred to a 15 mL centrifuge tube (Merck, CLS430791). After centrifugation at 1200 rpm for 5 min, cells were resuspended in CGM and counted using 10 µL of cell suspension in a Neubauer chamber. After establishing the concentration of the cells, the desired number of cells for each experiment was plated and allowed to adhere for 12 to 24 hours.

1.2. Drug treatments

MCF10A-ER-Src cells were plated in CGM in 6-well plates (Sarstedt, 83.3920) or T25 flasks (Sarstedt, 83.3910) and allowed to attach for at least 12 hours. The CGM was then replaced by restricted growth medium (restricted GM), composed of DMEM/F12, 0.5% CSHS, 0.5 µg/mL Hydrocortisone, 100 ng/mL Cholera toxin from Vibrio cholerae and 10 µg/mL Insulin and cells were left growing for 12 hours. Then, cells were treated with 1 µM 4-OH-TAM (Tamoxifen, Merck, H7904) to activate Src and induce transformation for the indicated timepoints. As control, MCF10A-ER-Src cells were treated with the same volume of vehicle absolute EtOH (EMSURE®, 1.00983) for the exact indicated timepoints.

1.3. FOXM1 RNA interference

To knock down FOXM1, two distinct small interference RNA (siRNA) were used. The siFOXM1 (Sigma-Aldrich, SASI_Hs01_00243977) knocks down all 4 FOXM1 isoforms. We also generated a siFOXM1 pool using the sequences previously published as specific against both FOXM1C and FOXM1A isoforms (Zhou et al., 2018), thereafter referred as siFOXM1C/A. To get a 50nM final concentration, 25nM of each siFOXM1C/A was used. The corresponding sequences of siFOXM1C/A pool are shown in Table 2.

Table 2. Sequences of siFOXM1C/A pool used for cell transfections.

siFOXM1C/A #1	5'-CCCAGGGUCUCCACAAUUG-3'
siFOXM1C/A #2	5'-AUUGCCCGAGCACUUGGAAUC-3'

To transfect cells, 250.000 cells were plated in T25 flasks in 3 mL of transfection medium composed of DMEM/F12, 0.5 µg/mL Hydrocortisone, 100 ng/mL Cholera toxin from Vibrio cholerae and 10 µg/mL Insulin and allowed to attach for at least 4 hours. Cells were then transfected with 50nM of siFOXM1 or siFOXM1C/A using 4 µL of Lipofectamine RNAiMAX (Invitrogen™, 13778) in Opti-MEM medium (Gibco™, 11058021) according to manufacturer's instructions. For western blot and PCR analysis, transfection medium was replaced after 12 hours by restricted GM, and cells were collected after 72 hours for protein or mRNA extractions. For FACS analysis, the transfection medium was replaced by CGM after 12 hours, and then after 24 hours, CGM was replaced by restricted GM for an additional 12 hours, prior to 4-OH-TAM or EtOH treatment for the indicated timepoint.

2. Immunofluorescence analysis

2.1. Src staining

75.000 cells were plated per well in a 6-well plate containing sterilized glass coverslips (VWR, 631-0150) coated with Poly-L-Lysine (Sigma, P78920) and treated for the indicated timepoints. After treatment, cells were rinsed with $PBS^{+/+}$ (0.18% $CaCl_2$ and 0.05% $MgCl_2$ in PBS1x) at pH7.2 and fixed for 10 min at room temperature (RT) in a fixative solution composed of 25% Formaldehyde Methanol-free (Sigma, 28908), 30% Piperazine-N,N'-bis(2-ethanesulfonic acid) 0.2M pH6.8 (Sigma, P6757), 15% 4-(2-hydroxyethyl)-1-piperazineethanesulfonic acid) 0.2M pH7 (Promega, H5302), 2% Ethylene glycol-bis(2-aminoethylether)-N,N,N',N' (EGTA) 0.5M pH6,8 (Sigma, E3889), 0.4% $MgSO_4$ 1M and MiliQ water. Following fixation, cells were washed with PBS1x and permeabilized with PBS+0.1% Triton-X100 (Sigma, T8787) for 2 min. Cells were then blocked for 1 h at RT using a blocking buffer at pH6.1, composed of 10mM MES pH6.1 (Sigma, M8250), 150 mM NaCl (Sigma, 31434), 5 mM EGTA pH6.8, 5mM $MgCl_2$, 5mM Glucose (Alfagene, LTI41965-039), 2% heat-inactivated Fetal Bovine Serum Premium (FBS) (Biowest, S008Y30304) and 1% Bovine Serum Albumin (BSA) (Sigma, A3294) in MiliQ water. Coverslips were then incubated overnight at 4°C with primary antibodies diluted in blocking buffer, including rabbit anti-pSrc (1/100, Invitrogen, 44-660G) and mouse anti-p120 catenin (1/100, BD Biosciences, 610133). The next day, following washes with PBS1x, the coverslips were incubated for 1 hour at RT with secondary antibodies in blocking buffer, including a FITC-conjugated anti-rabbit (1:200, Jackson ImmunoResearch, 711-095-152) and a Cy5-

conjugated anti-mouse (1:200, Jackson ImmunoResearch, 715-175-151), as well as with Rhodamine-conjugated phalloidin (Sigma, P-1951) at 0,3 mM. After 3 washes with PBS1x for 5 min, DNA was counterstained with 1 µg/ml DAPI (Sigma, D1377) for 10 min at RT. The coverslips were then washed with PBS1x for 5 min and mounted in Vectashield (Baptista Marques, H-1000). Leica SP5 confocal microscope (Leica Microsystems) was used to acquire fluorescence images and these images were analysed using the Fiji/ImageJ software.

2.2. FOXM1 staining

75.000 cells were plated per well in a 6-well plate containing sterilized glass coverslips coated with Poly-L-Lysine and treated for the indicated timepoints. Cells were fixed in freshly prepared 4% paraformaldehyde (Delta microscopies, 15713) in PBS1x for 20 min. After fixation, cells were rinsed in PBS1x and permeabilized for 7 min in PBS1x + 0.3% Triton-X100. After 1h blocking in 10% FBS in PBS-T (PBS + 0.05% Tween-20 (Sigma, p1379)), cells were incubated overnight at 4 °C with a rabbit anti-FOXM1 antibody (1:500, Proteintech, 13147-1-AP), diluted in PBS-T + 5% FBS. After washes with PBS-T, the coverslips were incubated for 1h at RT with the FITC-conjugated anti-rabbit secondary antibody (1:200 Jackson ImmunoResearch, 711-095-152) and with Rhodamine-conjugated phalloidin at 0,3 mM in PBS-T + 5% FBS. After washes with PBS-T, DNA was counterstained with 1 µg/ml DAPI for 10 min at RT. The coverslips were then washed with PBS1x for 5min and mounted in Vectashield. Zeiss AxioImager Z1 (Carl Zeiss) was used to acquire fluorescence images and these images were analysed using the Fiji/ImageJ software.

3. Real-time PCR

3.1. RNA Extraction and cDNA synthesis

75.000 cells were plated per well in a 6-well plate and treated for the indicated timepoints. After treatment, total RNAs were obtained using the Quick-RNA™ Microprep (Zymo Research, R1050) according to the manufacturer's instructions. RNA concentration was measured using Nanodrop 1000 (Thermo Fisher). 1 µg of total RNA was reverse-transcribed using the NZY First-Strand cDNA Synthesis Kit (NZYTech, MB125) according to the manufacturer's instructions.

3.2. PCR reaction

For PCR reactions, HOT FIREPol® DNA Polymerase (Solis Biodyne, 01-02-00500) kit was used. 1 µL of cDNA to a final concentration of 100 ng/µL or DNAse/RNAse-free water for the blank, was added to 9 µL of master mix (HOT FIREPol® 1x Buffer B1, 2.5 mM $MgCl_2$, 200 mM dNTP mix, 300 nM Forward Primer, 300 nM Reverse Primer and 0.5 U/ µL HOT

FIREPol® DNA Polymerase). Samples were placed in a thermocycler and the following program was used: 1 cycle for initial activation at 95ºC for 15 min; 35 cycles including a 30 sec step at 95ºC for denaturation, a 30 sec step at annealing temperatures corresponding to each set of primers (Table 3) and a 1 min step at 72ºC for extension. Lastly, a 5 min cycle at 72ºC was performed for final extension. Total volume of PCR products was mixed to 2 µL of Gel-red Nucleic acid gel stain (Biotium, 41003-T) with Loading dye (3 colours) and loaded onto a 2% agarose gel in TAE 1X (0.0489 mM Tris Base (VWR, 33621.260), 0.0037 mM EDTA and 1.14% Acetic Acid (VWR, 20108.292)). Sequences of primers specific to each FOXM1 isoform are shown in Table 3.

Table 3. Sequence of primers and their respective annealing temperatures used for PCR reactions.

Isoform	Primer sequences	Annealing temperature
FOXM1A	FW: 5'-GTCTCCACAATTGCCCGAG-3' RV: 5'-CCAAAATCTCGCAGATCGC-3'	52 ºC
FOXM1B	FW: 5'- GGTGTTTAAGCAGCAGAAACG-3' RV: 5'- CAGCACCTTGGGGGCAAT-3'	57 ºC
FOXM1C	FW: 5'-CCACTGGACCCAGGGTCTCC-3' RV: 5'-GCAGCACCTTGGGGGCAATGC-3'	61 ºC
FOXM1D	FW: 5'-CAGGTGTTTAAGCAGCAGA-3' RV: 5'-GGTGATGGGTGTACCAAAAT-3'	53.5 ºC
TBP	FW: 5'-GAGCCAAGAGTGAAGAACAGTC-3' RV: 5'-GCTCCCCACCATATTCTGAATCT-3'	59 ºC

3.3. Sanger sequencing

PCR products were purified using NZYGelpure kit (NZYtech, MB01101) according to manufacturer's instructions. The purified PCR products obtained using the specific primers for FOXM1A and FOXM1B were then sent for Sanger sequencing (Primer sequences listed in Table 3) at the i3S Genomics Scientific Platform. The sequences were analysed using the online tool BLAST to identify the FOXM1 isoforms.

3.4. RNA expression analysis (RT-qPCR)

RT-qPCR was performed in a C1000 Touch Thermal Cycler (CFX384 Real-Time System, Bio-Rad Laboratories). According to the manufacturer's instructions, samples were prepared on ice using iTaq™ Universal SYBR® Green Supermix (Bio-Rad, 172-5121). For each sample, a mastermix containing iTaq Universal SYBR Green Supermix (Bio-rad, 64361172) and of each primer (10µM) in MiliQ water was previously prepared. Each

reaction was analysed in duplicate with 9µL of mastermix and 1µL of cDNA 1µg/µL, or DNAse/RNAse-free water for the blank. The reactions were performed using the following conditions: 95ºC for 3 min, followed by 39 cycles including one 10 sec step at 95ºC, one 35 sec step at 59ºC, and melt curve from 55ºC to 95ºC with 0.5ºC increment for 10 sec. The primers for FOXM1B and FOXM1C used are listed in Table 3.

The $2^{-\Delta\Delta Ct}$ method was used to quantify the transcript levels of FOXM1B and FOXM1C against the transcript levels of the housekeeping gene, TATA-binding protein (TBP, primer sequences listed in Table 3). The CFX Manager Software (Bio-Rad Laboratories) was used to analyse the results.

4. Western blot analysis

For western blot analysis, 75.000 cells were plated per well in a 6-well plate and treated with EtOH or TAM for the indicated timepoints. To obtain whole cell protein extracts, cell pellets were resuspended in RIPA buffer [25 mM Tris•HCl pH 7.6, 150 mM NaCl, 1% NP-40, 1% sodium deoxycholate, 0.1% sodium dodecyl sulfate (SDS)] (Thermo Scientific, 89900), supplemented with protease inhibitors diluted at 1:100 (Thermo Scientific, 78440) and phosphatase inhibitors diluted at 1:100 (Thermo Scientific, 78420). After briefly vortexing, samples were sonicated in the Bioruptor® Plus (Diagenode) for 10 cycles at 4°C. Each cycle consisted of 20 sec at high power and 20 sec without sonication. The samples were then centrifuged at 13 300 rpm for 20 min at 4°C. Protein concentrations were determined by the Lowry Method (DC™ Protein Assay, Bio-Rad) according to the manufacturer's instructions.

Equal amounts of protein extracts in addition to the Precision Plus Kaleidoscope Standard molecular marker (Bio-Rad, 1610395) were then loaded in SDS-polyacrylamide gel electrophoresis and transferred onto Omniphobic Polyvinylidene Fluoride membranes (Amersham, 10600023) for western blot analysis. Membranes were then blocked with 5% non-fat dry milk in TBS-T (50 mM Tris-HCl pH7.4, 150 mM NaCl, 0.05% Tween-20) for 1h and incubated overnight at 4ºC with rabbit anti-FOXM1 C-terminal, hereby referred as FOXM1 C-term antibody (1:3000 Proteintech, 13147-1-AP) diluted in TBS-T supplemented with 2% non-fat milk or with rabbit anti-FOXM1 N-terminal, hereby referred as FOXM1 N-term antibody (1:1000 RayBiotech, 144- 02493) diluted in TBS-T supplemented with 3% non-fat milk and mouse anti-α-tubulin (1:10000 Sigma-Aldrich, T5168). The following day, membranes incubated with the FOXM1 C-term antibody or the FOXM1 N-term antibody were rinsed 3 times for 5 min with TBS-T supplemented with 2% or 3% non-fat milk, respectively. Membranes were then incubated with the secondary antibodies, including the IRDye® 800CW Donkey anti-rabbit IgG (LI-COR Biosciences, 925-32213) and IRDye®

680RD Donkey anti-mouse IgG (LI-COR Biosciences, 925-68072) diluted at 1:20 000 in TBS-T supplemented with 2% non-fat milk for the FOXM1 C-term antibody or 3% non-fat milk for the FOXM1 N-term antibody. Signals were detected using the Odyssey® CLx Infrared Imaging System (LI-COR Biosciences) and the Empiria® Studio software (LI-COR Biosciences) was used for quantitative analysis of protein levels (see the quantification section below).

5. Cell cycle profile analysis

MCF10A-ER-Src cells were plated, transfected without (Mock) or with siFOXM1 and treated for the indicated timepoint with EtOH or TAM, as described above. Cells were then collected in 5 mL round bottom polystyrene tubes (Corning, 352235) and centrifuged at 4°C for 5 min at 1000 rpm. The pellet was suspended in 1 mL FACS Buffer 1 (2% heat-inactivated Fetal Bovine Serum (Biowest, S181BH) in PBS1x, centrifuged again at 4°C for 5 min at 1000 rpm and then resuspended in 500 µL of FACS Buffer 1. Afterwards, cells were fixed with 500 µL of 70% Ethanol, added drop-by-drop while being gently vortexed, and incubated for 30 min at 4°C. After a centrifugation at 4°C for 5 min at 2000 rpm, cells were resuspended in 3 mL of PBS1x and incubated for 10 min on ice. A final centrifugation was performed at 4°C for 5 min at 2000 rpm before resuspending the pellet with 300 µL of FACS Buffer 2 (100 µg/mL RNAse A (Qiagen, 19101) and 20 µg/mL Propidium Iodide (Sigma, P4170) in PBS1x). Cells were incubated in a 37°C bath in the dark for 30 min and then filtered. Flow Cytometry was performed at low flow rate using a BD Accuri C6 Flow Cytometer (Becton-Dickinson, Franklin Lakes). FlowJo 10.7.1 software (Tree Star, Inc., Ashland) was used to analyse the cell cycle profile of each condition using the Watson Model (see the quantification section below).

6. Quantifications and Statistical analysis

6.1. FOXM1 immunostaining

The Fiji/ImageJ software was used to quantify the nuclear to cytoplasmic ratio of FOXM1 staining. Oval-shaped area selection tool of the same area was used to manually select the region of interest (ROI). The staining intensities of FOXM1 in nucleus and cytoplasm were measured using the Mean Gray value function, which is the sum of the gray values of all the pixels in the ROI divided by the number of pixels. After subtracting the background, we computed the ratio of nuclear to cytoplasmic FOXM1 staining of each cell quantified in each condition.

The Prism 9.0.0 software (GraphPad) was then used to conduct the statistical analysis. Normal distribution of the data was tested using a Shapiro–Wilk test. We used the Mann-Whitney non-parametric test to conduct the statistical comparison between EtOH or TAM

treated MCF10A-ER-Src cells for 6 and 24 hours. The data presented represents only one biological replicate and are shown as mean ± Standard Deviation (SD). ** indicates *p*-value<0.001. ns indicates $p > 0.05$.

6.2. RNA expression analysis

The CFX Manager Software (Bio-Rad Laboratories) was used to quantify FOXM1B and FOXM1C expression levels. The relative expression was calculated using the $2^{-\Delta\Delta Ct}$ method (Livak & Schmittgen, 2001). We obtained the fold changes in gene expression normalized to the expression of TBP, used as internal control, and relative to MCF10A-ER-Src cells treated with EtOH for the indicated timepoints.

The Prism 9.0.0 software (GraphPad) was then used to conduct the statistical analysis. We tested the normal distribution of the data using Shapiro–Wilk test. The statistical significance was calculated using One-way ANOVA. The data presented represent four independent biological replicates and are shown as mean ± SD. ns indicates $p > 0.05$.

6.3. Western blot analysis

The Empiria® Studio software (LI-COR Biosciences) was used to quantify the signal intensity of each band. Briefly, we imported the original files of western blot images from Image Studio software and then we executed the quantitative western blot antibody validation program in Empiria Studio software. The background was subtracted automatically when bands were quantified using the Adaptive Lane Finding process. We then verified that the ROI contained our bands of interest. Finally, we obtained the excel file of the signal intensity values of each band analysed. Fold changes in FOXM1 protein levels were calculated by normalizing the signal intensity of each band revealed by the anti-FOXM1 antibody in TAM-treated cells to the corresponding signal from the anti-α-Tubulin antibody, and to those of MCF10A-ER-Src cells treated with EtOH for the same time.

The Prism 9.0.0 software (GraphPad) was then used to conduct the statistical analysis. We tested the normal distribution of the data using Shapiro–Wilk test. The statistical significance was calculated using One-way ANOVA. The data presented represent five independent biological replicates and are shown as mean ± SD. ns indicates $p > 0.05$.

6.4. Cell cycle profile analysis

The FlowJo 10.7.1 software (Tree Star, Inc., Ashland) was used to analyse the cell cycle profile. Using gating, we selected the viable cell population based on their forward (FSC-A) and side scatter (SSC-A) properties (Figure 10A). Then, we excluded the doublets using the forward scatter height (FSC-H) vs. forward scatter area (FSC-A) density plot as

shown in Figure 10B below. And the cell cycle profile of the population of interest was analysed using the Watson model (Figure 10C).

The Prism 9.0.0 software (GraphPad) was then used to conduct the statistical analysis. We tested the normal distribution of the data using Shapiro–Wilk test. The statistical significance was calculated using One-way ANOVA. The data presented represent three independent biological replicates and are shown as mean ± SD. ** indicates *p*-value<0.001. *** indicates *p*-value<0.0001. ns indicates $p > 0.05$.

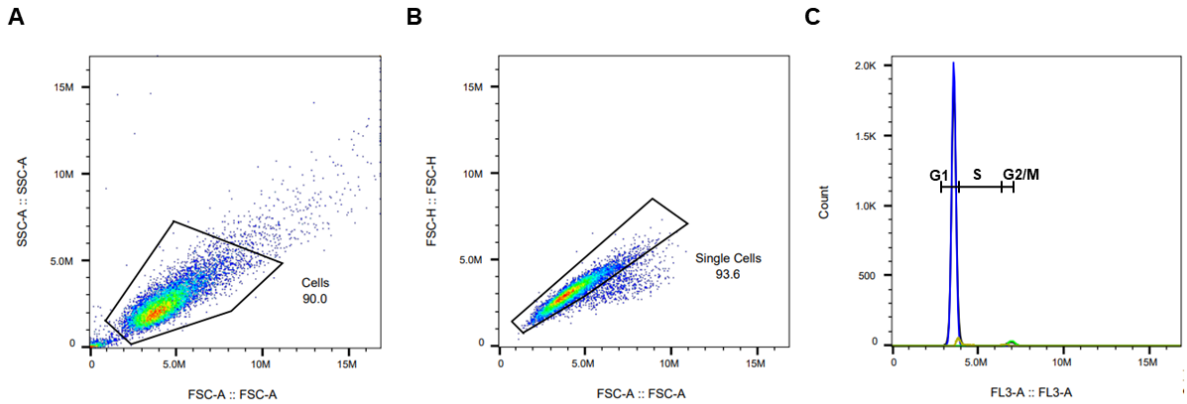

Figure 10. Cell cycle analysis using FlowJo software. (A) SSC-A vs FCS-A density plot. A gate has been applied to identify the viable cell population and to remove debris. Dead cells/debris have higher side scatter and lower forward scatter than living cells. (B) FSC-H vs FCS-A density plot. A gate has been applied to exclude the doublets from the single cell population. (C) Histogram of cell cycle profile representing G1, S and G2/M phases obtained using the univariate Watson model.

CHAPTER IV
RESULTS

1. FOXM1B and FOXM1C are two major isoforms significantly upregulated in human carcinomas

We raised three key questions described in Chapter II, to assess our hypotheses and to investigate the role of different FOXM1 isoforms and truncated forms in basal-like breast cancer.

Regarding the first question, to distinguish between FOXM1 isoforms' tumour suppressor and oncogenic roles and to get insight into which FOXM1 isoforms could be implicated in breast cancer cell tumorigenesis and could enhance oncogenic role during cellular transformation, we used the ISOexpresso database (wiki.tgilab.org/ISOexpresso) to identify the FOXM1 isoforms differentially expressed between normal tissues and human carcinomas. ISOexpresso database identified in total five spliced variants of FOXM1: FOXM1A, FOXM1B, FOXM1C along with two isoforms previously described as FOXM1b1 and FOXM1b2. FOXM1b1 and FOXM1b2 have been shown to have a structural similarity to FOXM1B; FOXM1b1 has a GCA deletion (amino acid 168) and CAG insertion (amino acid 327), whereas FOXM1b2 has only the GCA deletion (X. Kong et al., 2013), hence we grouped these three isoforms together and referred to them as FOXM1B.

Over a total of 1097 Breast Invasive carcinoma (BIC) samples, the expression levels of FOXM1A, FOXM1B and FOXM1C were considerably higher than those of normal samples (n=114). FOXM1A expression exhibited a 0.3-fold increase in median transcript per million (TPM) when compared to normal samples, whereas FOXM1B showed a 17-fold increase and FOXM1C showed a 10-fold increase (**Figure 11**). According to ISOexpresso database, only isoforms whose expression shows a median TPM fold change greater than 2 are significantly altered (I. S. Yang et al., 2016). Therefore, FOXM1B and FOXM1C were identified to be the two major isoforms overexpressed in BIC tumour samples in comparison to normal samples.

We also analysed the expression levels of FOXM1 isoforms in other types of human carcinomas, including Lung Squamous carcinoma (LSC), Bladder Urothelial carcinoma (BUC), Colon adenocarcinoma (CA), Lung adenocarcinoma (LA) and Prostate adenocarcinoma (PA) (**Figure 11**). BUC, CA and LA exhibited FOXM1B and FOXM1C overexpression similarly to BIC. LSC additionally exhibited a 2.8-fold increase in FOXM1A median TPM in comparison to normal samples. Only PA showed no significant changes in expression levels of FOXM1A, FOXM1B and FOXM1C.

In conclusion, the ISOexpresso *in silico* analysis revealed that FOXM1B and FOXM1C are the two main isoforms significantly overexpressed in BIC and most other types of human carcinomas. FOXM1A is only significantly upregulated in Lung Squamous carcinoma.

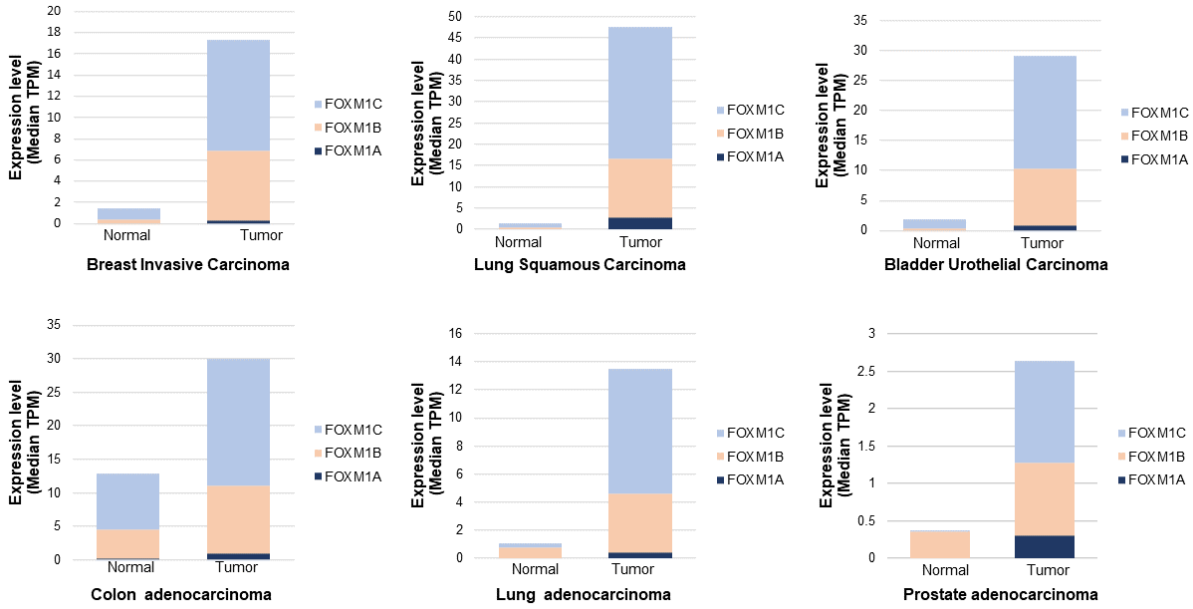

Figure 11. FOXM1B and FOXM1C are two major splice variants that are significantly upregulated in tumour samples. FOXM1 transcripts expression levels calculated using median transcripts per million (TPM) in several types of human cancer tissues in comparison to normal tissues, data from ISOexpresso (wiki.tgilab.org/ISOexpresso).

2. MCF10A-ER-Src cells treated with tamoxifen acquire cellular transformation traits

Breast cancer was and remains to be one of the most prevalent types of cancer among women (Sung et al., 2021), and according to ISOexpresso database, FOXM1 isoforms are significantly upregulated in BIC. In addition to this, Janody's lab gathered preliminary data suggesting that FOXM1 transiently accumulates in pre-malignant MCF10A-ER-Src cells. Therefore, using this inducible MCF10A-ER-Src cell model, which recapitulates molecular events taking place during breast cancer onset, offers the advantage to address the role of distinct FOXM1 isoforms and/or their truncated forms, and how they are re-activated during the early stages of breast carcinogenesis.

As described previously in the introduction, MCF10A-ER-Src cell model undergoes cellular transformation upon treatment with TAM, contrary to cells treated concurrently with the vehicle EtOH (Tavares et al., 2017). During the first 12 hours of TAM treatment, cells maintain an epithelial-like morphology and accumulate polarized acto-myosin stress fibres. However, 24 hours after TAM treatment, these cells lose the polarized acto-myosin stress fibres and undergo EMT, characterized by the disassembly of AJs. To confirm that this

inducible cell model behaves likewise, we performed immunofluorescence (IF) analysis using phalloidin, which stains actin filaments, DAPI to stain the nucleus and antibodies against p120-catenin (p120ctn) to identify AJs and against the phosphorylated form of Src (pSrc) to observe the activity of ER-Src and endogenous pSrc, in cells treated with EtOH or TAM for 6 or 24 hours (**Figure 12**). This part of the project was performed in collaboration with Alice Eon.

In MCF10A-ER-Src cells treated with EtOH for 6 and 24 hours, we observed p120ctn to be present at cell-cell junctions, indicating that cells maintained their epithelial features. We also observed a well-ordered organization of F-actin and pSrc to be mainly localized at the cell edges as expected for untransformed cells (**Figure 12**).

In cells treated with TAM compared to cells treated with vehicle EtOH, the F-actin network showed pronounced alterations. At 6 hours after TAM treatment, MCF10A-ER-Src cells displayed higher F-actin levels, and 24 hours after TAM treatment, cells showed a complete disorganization of F-actin as expected. In MCF10A-ER-Src cells treated with TAM for 6 hours, we observed the presence of p120ctn at cell-cell junctions, indicating an epithelial-like phenotype. However, 24 hours after TAM treatment, cells lost their connection and failed to accumulate p120ctn at the cell membrane, suggestive of a mesenchymal phenotype. Although we did not observe main differences in pSrc levels between TAM and EtOH-treated cells, pSrc appeared to re-localize in TAM-treated cells. pSrc localized to the cytoplasm 6 hours after TAM treatment and then, accumulated around the nucleus 24 hours after TAM treatment (**Figure 12**).

Considering all these observations, we can confirm that TAM-treated MCF10A-ER-Src cells undergo morphological cellular transformation.

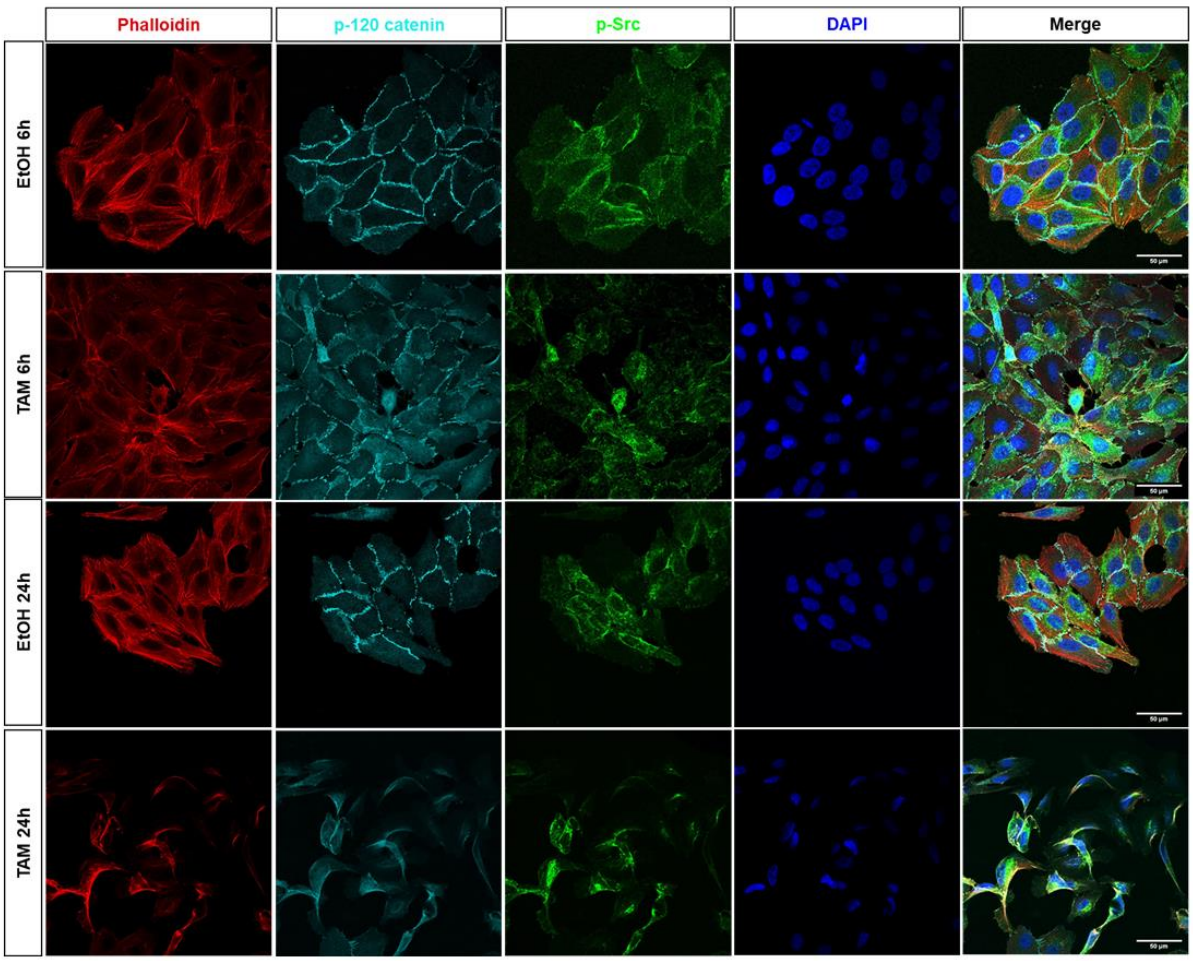

Figure 12. MCF10A-ER-Src cells acquire cellular transformation characteristics upon treatment with TAM. Standard confocal sections acquired using 63X objective, of MCF10A-ER-Src cells treated with EtOH or TAM for 6 or 24 hours, stained with Phalloidin (red) to visualize F-actin, DAPI (blue) to stain the nuclei and antibodies against pSrc (green) to observe Src activity and p120-catenin (Cyan) to identify adherens junctions. Scale bars represent 50µm.

3. FOXM1A, FOXM1B and FOXM1C are the three FOXM1 isoforms expressed in untransformed MCF10A-ER-Src cells

After the validation of MCF10A-ER-Src model, we initially identified which FOXM1 isoforms were expressed in untransformed MCF10A-ER-Src cells to subsequently investigate if their expression changed during cellular transformation. We performed endpoint PCR and agarose gel electrophoresis using previously described primers (X. Zhang, Zhang, et al., 2017) specific for each FOXM1 isoform. FOXM1A contains both alternative exons, VA and VIIA, therefore the forward primer was designed to anneal in a region of exon VA, and the reverse primer was designed to anneal in a region of exon VIIA (primers are represented by red arrows in **Figure 13A**). FOXM1B does not encompass any of the alternative exons, hence the forward primer was designed to anneal at the junction of exon V and exon VI, and the reverse primer was designed to anneal at junction of exon

VII and exon VIII (Primers are represented by red arrows in **Figure 13B**). FOXM1C only retains exon VA, therefore the forward primer was designed to anneal in a region of exon VA, whereas reverse primer was designed to anneal at the junction of exon VII and exon VIII (Primers are represented by red arrows in **Figure 13C**). FOXM1D only retains exon VIIA, so the forward primer was designed to anneal at the junction of exon V and exon VI, and the reverse primer was designed to anneal in the region of exon VIIA (Primers are represented by red arrows in **Figure 13D**).

HCT-116, a human colon cancer cell line, that has been demonstrated to express all FOXM1 isoforms was employed as a positive control (X. Zhang, Zhang, et al., 2017). To evaluate any possible DNA contamination in samples, we included blanks (no template control) per pair of FOXM1 isoform specific primers. None of our blanks showed any bands, confirming that all our samples were free of extraneous nucleic acid contamination (Figure **13A, B, C, D**). A band at 345bp was amplified using FOXM1A specific PCR primers in HCT-116 cells and in untreated MCF10A-ER-Src cells, which is the expected size of the PCR product for FOXM1A (**Figure 13A**). A band at 263bp was amplified using FOXM1B specific PCR primers in HCT-116 cells and in untreated MCF10A-ER-Src cells, which is the expected size of the PCR product for FOXM1B (**Figure 13B**). A band at 298bp was amplified using FOXM1C specific PCR primers in HCT-116 cells and in untreated MCF10A-ER-Src cells, which is the expected size of the PCR product for FOXM1C (**Figure 13C**). A band at 343bp was amplified using FOXM1D specific PCR primers in HCT-116 cells, which is the expected size of the PCR product for FOXM1D, however in untreated MCF10A-ER-Src cells we only observed a smear and no band at 343bp (**Figure 13D**). These observations suggested that the observed bands represent different FOXM1 isoforms.

To validate that the products amplified by each of the FOXM1-specific primers in untreated MCF10A-ER-Src cells were different FOXM1 isoforms, we tested whether the observed bands would go down if all FOXM1 isoforms were knocked down using siRNA directed against the domain encoding the TAD domain. Knocking down FOXM1 has been shown to decrease cell proliferation and induce cell cycle arrest (Feng et al., 2018, ; Wu et al., 2010), hence we expected a reduction in number of cells transfected with siFOXM1. Accordingly, brightfield images showed that siFOXM1 transfected MCF10A-ER-Src cells appeared less confluent, compared to those that were transfected without siFOXM1 (**Figure 13E**). In cells knocked down for siFOXM1, we did not detect any PCR product amplified at the expected sizes for FOXM1A (**Figure 13A**), FOXM1B (**Figure 13B**), FOXM1C (**Figure 13C**) and FOXM1D (**Figure 13D**) using the FOXM1-specific primers, hence confirming that the bands amplified in HCT-116 and untreated MCF10A-ER-Src cells represent different

FOXM1 isoforms. These results suggest that untransformed MCF10A-ER-Src cells express FOXM1A, FOXM1B, FOXM1C but not FOXM1D.

We then investigated whether the observed bands amplified using the FOXM1A and FOXM1C primers, but not the FOXM1B primers, would go down if we knock down only the isoforms FOXM1A and FOXM1C, using a siRNA directed against the alternative exon VA (thus referred to as siFOXM1C/A). Brightfield images showed that siFOXM1C/A transfected MCF10A-ER-Src cells appeared less confluent in comparison to transfection controls (**Figure 13E**), suggesting the knockdown of FOXM1 isoforms. As expected, in MCF10A-ER-Src cells transfected with siFOXM1C/A, no detectable PCR products were amplified using the FOXM1A- (**Figure 13A**) and FOXM1C- (**Figure 13C**) specific primers. Surprisingly, we could not detect either any PCR product in these cells using the FOXM1B-specific primers (**Figure 13B**). These observations suggest three scenarios: (1) - The siFOXM1C/A is not specific; hence it is not only targeting FOXM1A and FOXM1C, but also FOXM1B. (2) – There is a mechanism through which the expression of FOXM1B likewise decreases when FOXM1A or FOXM1C expression goes down. (3) – The primers we are using for FOXM1A or FOXM1B are not specific, and they are amplifying FOXM1C.

To distinguish between these three possibilities, we sent the PCR products obtained using the specific primers for FOXM1A and FOXM1B for Sanger sequencing to validate FOXM1A and FOXM1B primers. The Sanger sequencing data on FOXM1A and FOXM1B PCR primers was then analysed using BLAST online tool, which indicated that the primers were amplifying specifically FOXM1A (**Annex Figure 1A**) and FOXM1B (**Annex Figure 1B**). These findings indicated that siFOXM1C/A may not be specific or that there may be a mechanism by which FOXM1B expression decreases in response to FOXM1C or FOXM1A knockdown.

Taking into account all the prior observations, we concluded that PCR primers were specifically amplifying different FOXM1 isoforms. And FOXM1A, FOXM1B and FOXM1C are the three main FOXM1 transcript variants expressed in untransformed MCF10A-ER-Src cells.

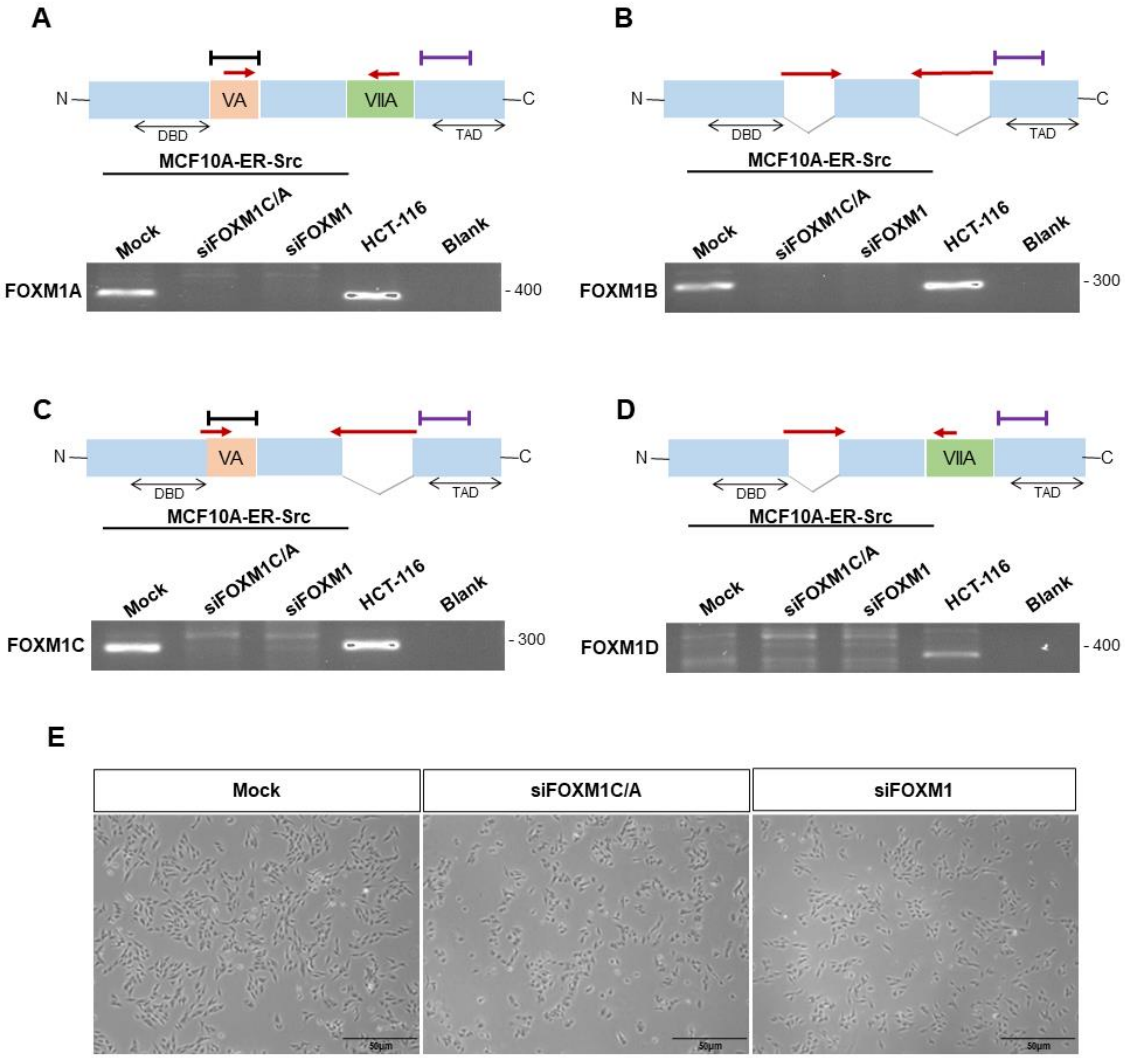

Figure 13. FOXM1 isoform-specific primers identify FOXM1A, FOXM1B and FOXM1C as being expressed in the untransformed MCF10A-ER-Src cell line. (A) PCR products amplified using specific primers for FOXM1A. (B) PCR products amplified using specific primers for FOXM1B. (C) PCR products amplified using specific primers for FOXM1C. (D) PCR products amplified using specific primers for FOXM1D. The expression of all FOXM1 isoforms in untransformed MCF10A-ER-Src cells (Mock), cells transfected with siFOXM1C/A, cells transfected with siFOXM1, was determined using endpoint PCR, where HCT-116 cell line was used as positive control. Blank was used as control for any possible DNA contaminations. Red arrows in the cartoon illustration of FOXM1 isoforms represent the annealing position of each primer used in endpoint PCR, black icon represents the domain targeted by siFOXM1C/A and purple icon represents the domain targeted by siFOXM1 used for transfection in MCF10A-ER-Src cells. (E) Brightfield images of MCF10A-ER-Src cells transfected without (Mock) and with siFOXM1 or siFOXM1C/A. Images were acquired with a 5X objective. Scale bars represent 50µm.

4. FOXM1B and FOXM1C expression levels are not affected in MCF10A-ER-Src cells during the first 24 hours of TAM-treatment

To investigate how does FOXM1 becomes oncogenic and which isoforms could be transiently upregulated to sustain pre-malignant features, including proliferation or an inflammatory microenvironment, through their TAD domain, we performed RT-qPCR analysis. According to the ISOexpresso *in silico* analysis, we predicted that FOXM1B and/or FOXM1C could be transiently upregulated in pre-malignant MCF10A-ER-Src cells. Therefore, we investigated whether FOXM1B and FOXM1C mRNA levels were affected in pre-malignant MCF10A-ER-Src cells compared to untransformed MCF10A-ER-Src cells. We used FOXM1 isoform-specific primers to perform RT-qPCR analysis on RNA isolated from MCF10A-ER-Src cells treated with TAM or EtOH for 2, 6, 12 and 24 hours. The mRNA levels of FOXM1B and FOXM1C on extracts from MCF10A-ER-Src cells treated with TAM for 2, 6, 12 and 24 hours were normalised to the expression level of TBP, used as internal control, and to those of MCF10A-ER-Src cells treated with EtOH for the same timepoints.

Surprisingly, the fold-change in expression of FOXM1B and FOXM1C in all four biological replicates was not significantly affected in MCF10A-ER-Src cells treated with TAM at all timepoints analysed, compared to those treated with EtOH for the same time (**Figure 14A**). Yet, brightfield images of cells treated with EtOH or TAM at each time point for each biological replicate indicated that TAM-treated cells underwent morphological changes associated with cellular transformation. While EtOH-treated cells maintained an epithelial-like morphology during the 24 hours of treatment, TAM-treated cells, however, detached from the substrate 24 hours after treatment (**Figure 14B**).

These findings indicated that the expression of the FOXM1B and FOXM1C isoforms is not affected in MCF10A-ER-Src cells during the first 24 hours of TAM treatment.

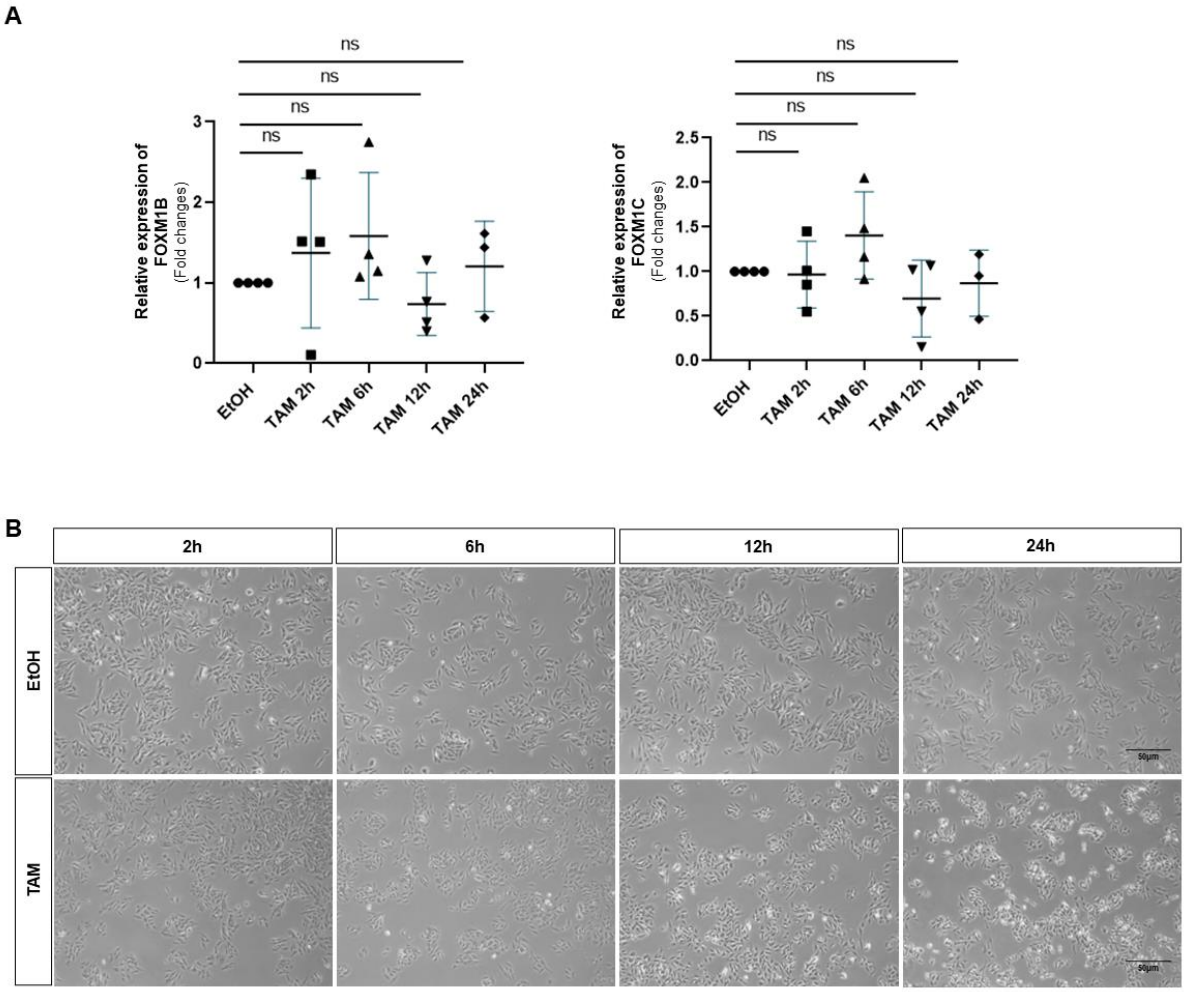

Figure 14. FOXM1B and FOXM1C mRNA levels are not affected in MCF10A-ER-Src cells during the first 24 hours of TAM-treatment. (A) Quantifications from four biological replicates of FOXM1B (left panel) and FOXM1C (right panel) mRNA levels on extracts from MCF10A-ER-Src cells treated with TAM for 2, 6, 12 and 24 hours, normalised to those of TBP used as house-keeping gene and to those of MCF10A-ER-Src cells treated with EtOH for the same timepoints. Statistical analysis was calculated using one-way ANOVA test. The data are means ± SD. ns indicates p-value >0.05. (B) Brightfield images acquired with 5X objective of MCF10A-ER-Src cells treated with EtOH or TAM for 2, 6, 12 and 24 hours. Scale bars represent 50µm.

5. FOXM1 do not accumulate in MCF10A-ER-Src cells during the first 24 hours of TAM treatment

In the previous results, we found out that the expression of the FOXM1B and FOXM1C isoforms is not affected in pre-malignant MCF10A-ER-Src cells. We therefore tested if Src activation stabilizes FOXM1 by promoting a transient accumulation of F-actin or cleave FOXM1 through ERK activation.

To assess this hypothesis, we performed western blot analysis using a rabbit polyclonal antibody against the C-terminal region common to all FOXM1 isoforms (hence referred to as FOXM1 C-term). We expected that the FOXM1 C-term antibody would reveal 2 bands

of higher intensity in MCF10A-ER-Src cells treated with TAM for 6 or 12 hours. One band at around 110kDa that would reveal full-length FOXM1B and/or FOXM1C, while a band at around 85kDa would disclose the cleaved form of FOXM1C lacking the N-terminal domain. Membranes were also blot with an anti-α-tubulin antibody used as loading control. To first ascertain the specificity of the FOXM1 C-term antibody, we performed a western blot using protein extracts from MCF10A-ER-Src cells transfected without (Mock) and with siFOXM1 that knocks down all FOXM1 isoforms. The FOXM1 C-term antibody revealed 2 main bands at around 120kDa and 100kDa in Mock MCF10A-ER-Src cells. However, only the band at around 100kDa was reduced in MCF10A-ER-Src cells knocked down for FOXM1 (**Figure 15A**). Quantifications of the intensity levels of the band at around 100kDa indicated that it was reduced by ~80% in siFOXM1 MCF10A-ER-Src cells in comparison to the Mock (**Figure 15B**). Hence, this band most likely represents full-length FOXM1 (FOXM1 FL). We then tested if the FOXM1 protein levels were affected during cellular transformation using protein extracts from MCF10A-ER-Src cells treated with EtOH or TAM for 2, 6, 12, and 24 hours by western blotted with C-term antibody. Surprisingly, the levels of the bands at around 100kDa revealed by the anti-FOXM1 C-term antibody were not significantly altered between EtOH and TAM treated cells for all the timepoints (**Figure 15C and D**). Moreover, we did not observe the presence of additional bands in TAM-treated cells, compared to those treated with EtOH for the same time (**Figure 15C**).

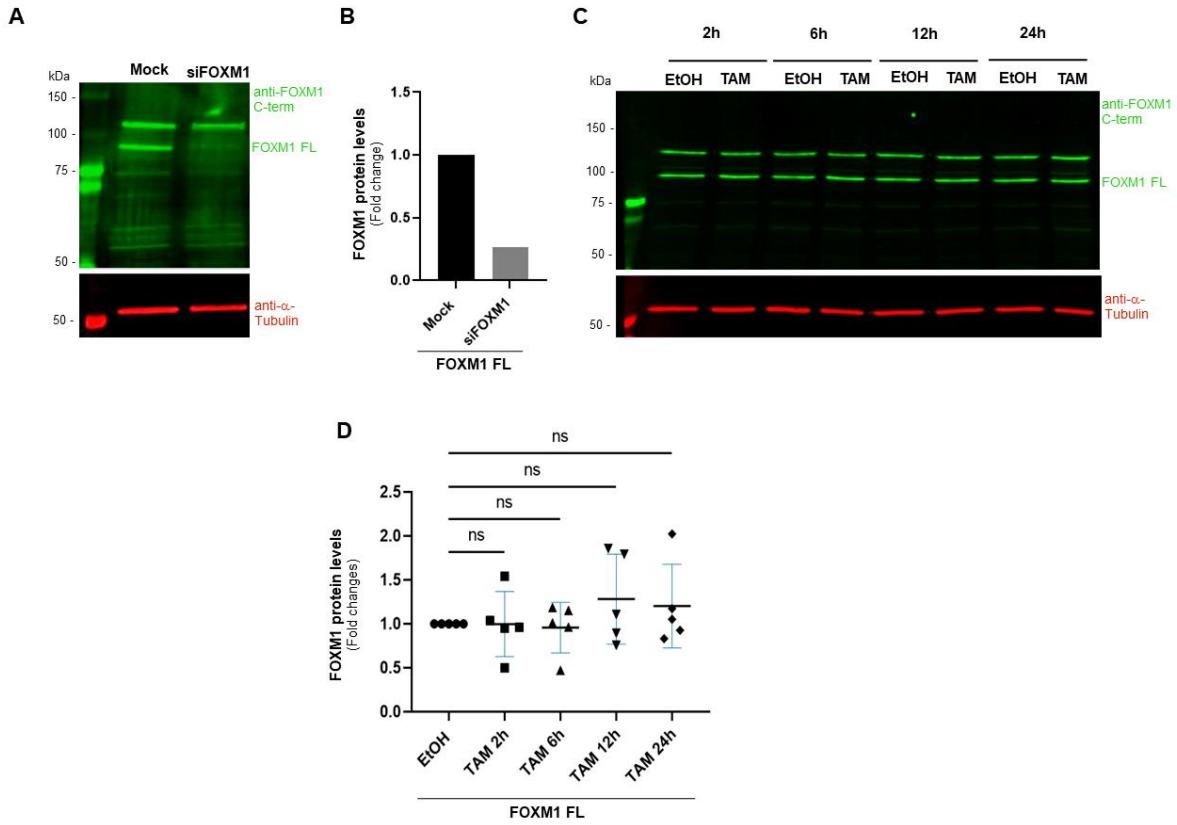

Figure 15. An anti-FOXM1 antibody directed against the C-terminal domain reveals no difference in FOXM1 levels in MCF10A-ER-Src cells during the first 24 hours of TAM treatment. (A) Western blot on protein extracts from MCF10A-ER-Src cells transfected without (Mock) or with siFOXM1, blotted with the anti-FOXM1 C-term antibody (green) and with the anti-α-tubulin (red) used as loading control. (B) Quantification of the intensity levels of the band at around 100kDa (FOXM1 FL) revealed by the anti-FOXM1 C-term antibody MCF10A-ER-Src cells transfected without (Mock) and with siFOXM1, normalized to the corresponding α-tubulin. (C) Western blot on protein extracts from MCF10A-ER-Src cells treated with EtOH or TAM for 2, 6, 12 and 24 hours, blotted with the anti-FOXM1 C-term antibody (green) and with the anti-α-tubulin antibody (red) used as loading control. (D) Quantification from five biological replicates of the ratio of FOXM1 FL revealed by the anti-FOXM1 C-term antibody between MCF10A-ER-Src cells treated with TAM for 2, 6, 12 and 24 hours and those treated with EtOH for the same time, normalized to the corresponding α-tubulin. Statistical significance was calculated using one-way ANOVA test. The data are means ± SD. ns indicates *p*-value > 0.05.

To further confirm that Src activation does not affect FOXM1 protein levels, we performed the same western blot analysis using a rabbit polyclonal antibody directed towards the N-terminal region, present in all FOXM1 isoforms (hence referred to as FOXM1 N-term). We expected that FOXM1 N-term antibody would reveal a band of higher intensity at around 110kDa (FOXM1 FL) in MCF10A-ER-Src cells. Membranes were also blot with an anti-α-tubulin antibody used as loading control. These experiments were performed in collaboration with Alice Eon.

We first confirmed the specificity of the anti-FOXM1 N-term antibody by analysing the pattern of bands in Western blot revealed by this antibody between protein extracts from MCF10A-ER-Src cells transfected without (Mock) and with siFOXM1 that knocks down all FOXM1 isoforms. In Mock MCF10A-ER-Src cells, the anti-FOXM1 N-term antibody revealed 3 main bands at around 100kDa, 50kDa, and 25kDa. In MCF10A-ER-Src protein extracts knocked down for FOXM1, the intensity levels of the two bands at around 100kDa and 50kDa were reduced, suggesting that these two bands identify two forms of FOXM1 (**Figure 16A**). Quantifications indicated that the intensity of these bands were reduced by ~70% in siFOXM1 MCF10A-ER-Src cells when compared to Mock cells (**Figure 16B**). The band at around 100kDa most likely identifies full-length FOXM1 FL, which was also revealed by the anti-FOXM1 C-term antibody, while the band at around 50kDa might represent a truncated form of FOXM1 (FOXM1 TF).

We then analysed if the levels of the two FOXM1-specific bands revealed by the anti-FOXM1 N-term antibody were altered during transformation of the MCF10A-ER-Src cell line by comparing their levels in cells treated with EtOH or TAM for 2, 6, 12 or 24 hours by Western blot. Quantification of the intensity levels of the band at around 100kDa indicated that full-length FOXM1 protein was not significantly altered between cells treated with EtOH and TAM at any timepoints (**Figure 16C and D**), thus confirming our previous observations using the anti-FOXM1 C-term antibody. Also, quantification of the intensity levels of the band at around 50kDa (FOXM1 TF) showed that the levels of this truncated form was not

significantly altered in TAM-treated cells, when compared to those treated with EtOH for the same time (**Figure 16C and E**). In addition, we did not observe the presence of additional bands in TAM-treated cells, compared to those treated with EtOH for the same time (**Figure 16C**).

In conclusion, Src-induced cellular transformation does not seem to impact on FOXM1 levels, nor does it appear to trigger FOXM1 cleavage.

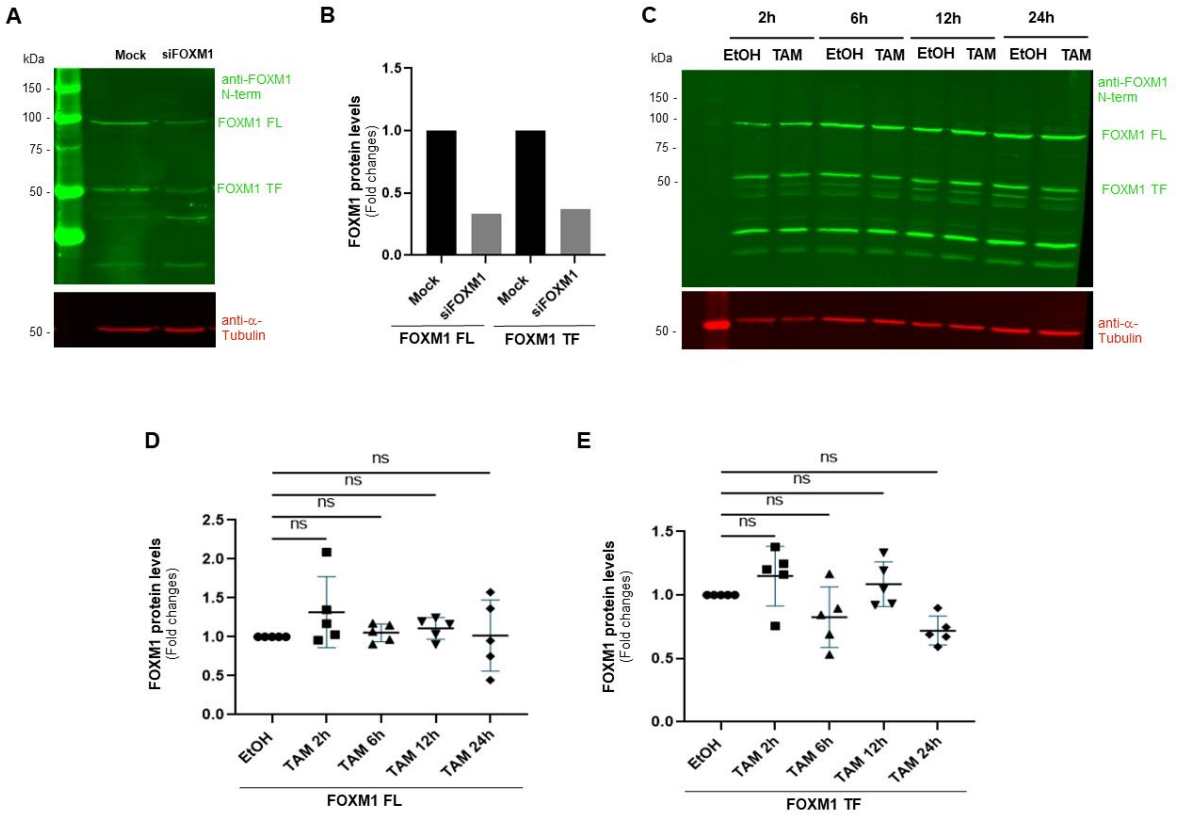

Figure 16. An anti-FOXM1 antibody directed against the N-terminal domain reveals no difference in FOXM1 levels in MCF10A-ER-Src cells during the first 24 hours of TAM treatment. (A) Western blot on protein extracts from MCF10A-ER-Src cells transfected without (Mock) or with siFOXM1, blotted with the anti-FOXM1 N-term antibody (green) and with the anti-α-tubulin antibody (red), used as loading control. (B) Quantification of the intensity levels of the ~100kDa (FOXM1 FL) and ~50kDa (FOXM1 TF) bands revealed by the anti-FOXM1 N-term antibody in MCF10A-ER-Src cells transfected without (Mock) and with siFOXM1, normalized to those of the corresponding α-tubulin level. (C) Western blot on protein extracts from MCF10A-ER-Src cells treated with EtOH or TAM for 2, 6, 12 and 24 hours, blotted with the anti-FOXM1 N-term antibody (green) and with the anti-α-tubulin antibody (red), used as loading control. (D) Quantification from four biological replicates of the ratio of FOXM1 FL revealed by the anti-FOXM1 N-term antibody between MCF10A-ER-Src cells treated with TAM for 2, 6, 12 and 24 hours and those treated with EtOH for the same time, normalized to the corresponding α-tubulin (E) Quantification from four biological replicates of the ratio of FOXM1 TF revealed by the anti-FOXM1 N-term antibody between MCF10A-ER-Src cells treated with TAM for 2, 6, 12 and 24 hours and those treated with EtOH for the same time, normalized to the corresponding α-tubulin. Statistical significance was calculated using one-way ANOVA test. The data are means ± SD. ns indicates *p*-value > 0.05.

6. FOXM1 transiently accumulates in the nucleus of pre-malignant MCF10A-ER-Src cells

Our observations indicate that during the first 24 hours of TAM treatment, the expression of FOXM1B and FOXM1C is not affected in MCF10A-ER-Src cells (**Figure 14**). Also, full length FOXM1 is not stabilized in these cells. Moreover, we did not find evidence that TAM-treatment triggers the cleavage of full length FOXM1 (**Figure 15 and 16**). Hence, these data suggest that Src activation does not stabilize FOXM1 by promoting actin filament accumulation, nor does it cleave FOXM1 through ERK activation. Yet, these observations do not exclude the possibility that Src potentiates FOXM1 transcriptional activity. To test this hypothesis, we analysed if FOXM1 re-localizes to the nucleus in MCF10A-ER-Src cells upon treatment with TAM by IF. MCF10A-ER-Src cells treated with EtOH or TAM for 6 or 24 hours were stained with the anti-FOXM1 C-term antibody to observe FOXM1 localization, phalloidin, which stains actin filaments and DAPI to stain the nucleus. We observed that in cells treated with EtOH for 6 and 24 hours, only a few cells showed a strong nuclear accumulation of FOXM1. Some of these appeared to undergo cell division, as we could observe them in the process of cytokinesis (see insert in **Figure 17A**). In contrast, nearly all cells treated with TAM for 6 or 24 hours exhibited nuclear accumulation of FOXM1 (**Figure 17A**).

To quantify these observations, we evaluated the nuclear to cytoplasmic FOXM1 signal ratio in MCF10A-ER-Src cells treated with TAM for 6 or 24 hours compared to those of cells treated with EtOH for the same time. The quantification represents only one biological replicate; however, in each condition a minimal number of 50 cells was evaluated. Statistical significance was calculated using the Mann-Whitney non-parametric test. We were expecting to see no difference in nuclear to cytoplasmic ratio of FOXM1 signal in MCF10A-ER-Src cells treated with EtOH, but unexpectedly the nuclear to cytoplasmic ratio of FOXM1 signal of MCF10A-ER-Src treated with EtOH for 24 hours showed a significant increase when compared to MCF10A-ER-Src cells treated with EtOH for 6 hours. The nuclear to cytoplasmic ratio of FOXM1 signals showed a significant increase in cells treated with TAM for 6 hours when compared to those treated with EtOH for the exact same time. In contrast, the nuclear to cytoplasmic FOXM1 signal ratio was not significantly different between cells treated with TAM for 24 hours and those treated with EtOH for the same time (**Figure 17B**). Also, the nuclear to cytoplasmic ratio of FOXM1 signal was not significantly different between MCF10A-ER-Src cells treated with TAM for 6 hours and for 24 hours.

Thus, these preliminary data suggest that Src activation induces the transient nuclear translocation of FOXM1 in pre-malignant MCF10A-ER-Src.

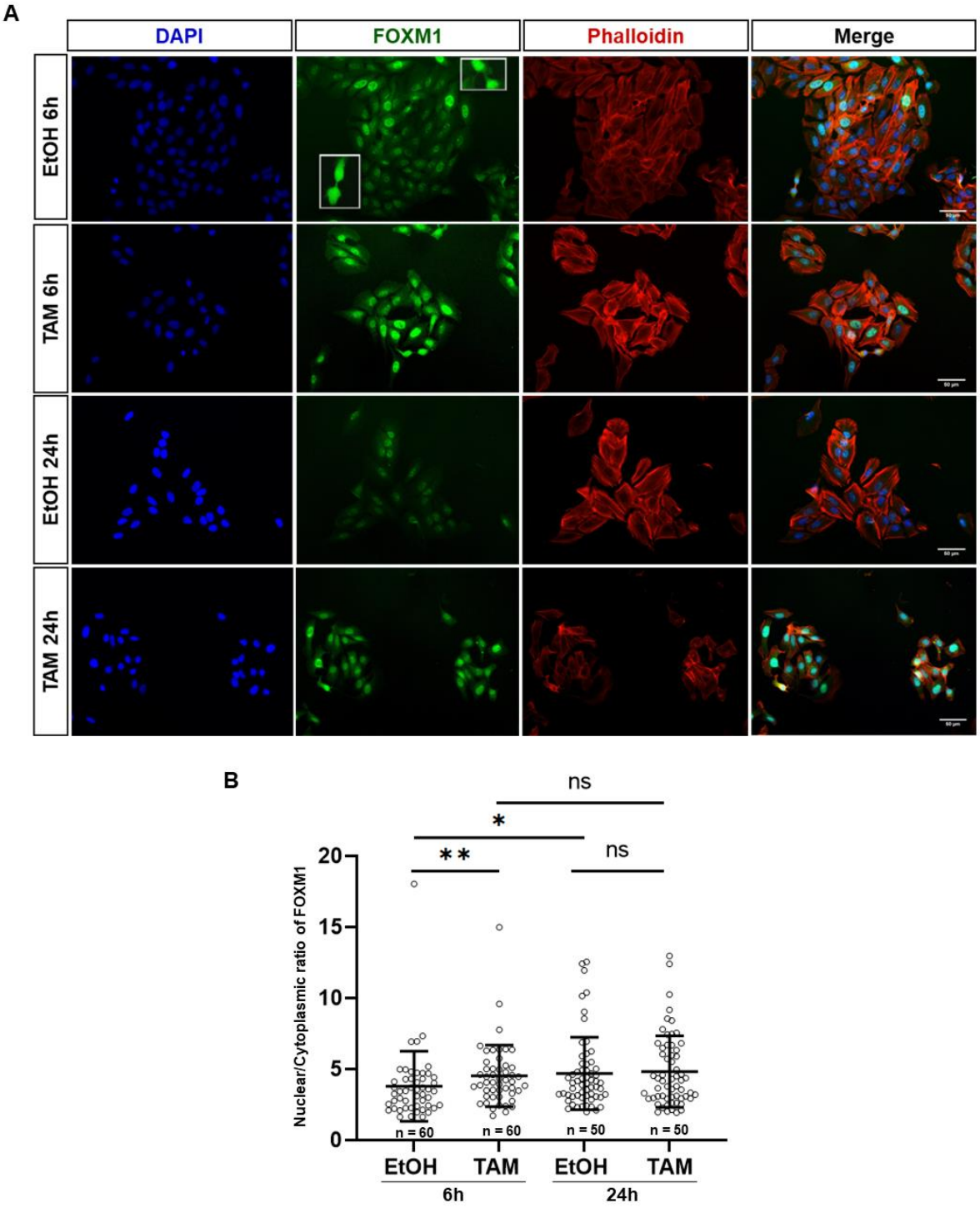

Figure 17. FOXM1 might transiently re-localize to the nucleus in pre-malignant MCF10A-ER-Src cells. (A) Standard fluorescent images of MCF10A-ER-Src cells treated with EtOH or TAM for 6 or 24 hours, stained with Phalloidin (red) to visualize F-actin, DAPI (blue) to stain the nuclei and anti-FOXM1 C-term (green) to observe FOXM1 localization. Scale bars represent 50µm. **(B)** Nuclear to cytoplasmic FOXM1 signal ratio in MCF10A-ER-Src cells treated with EtOH or TAM for 6 or 24 hours. Each dot represents the quantification of one cell. Data are from one biological replicate. Statistical significance was calculated using Mann-Whitney non-parametric t-test. The data are means ± SD. ** *p*-value <0.001, * *p*-value <0.05, ns *p*-value >0.05.

7. FOXM1 might be required to sustain the proliferation of TAM-treated MCF10A-ER-Src cells

As FOXM1 appears to transiently accumulate in the nucleus of pre-malignant MCF10A-ER-Src cells, we examined the effect of knocking down FOXM1 on the ability of pre-malignant MCF10A-ER-Src to sustain proliferation. MCF10A-ER-Src cells were transfected without (Mock) and with siFOXM1 that knocks down all FOXM1 isoforms for 48 hours before treating them with EtOH or TAM for 24 hours in the absence of EGF and low concentration serum. We expected that knocking down all FOXM1 isoforms prior Src-induced oncogenic transformation would reduce the number of cells in S-phase of the cell cycle quantified by cell cycle profile analysis.

Brightfield images showed that EtOH or TAM-treated cells transfected with siFOXM1 appeared to be less confluent than those transfected without siFOXM1 (Mock), suggesting a role of FOXM1 in promoting proliferation (**Figure 18A**). As previously reported (Tavares et al., 2017), TAM-treated MCF10A-ER-Src cells transfected without siFOXM1 showed a significant increase in the percentage of cells in S-phase of the cell cycle compared to Mock cells treated with EtOH for the same time (**Figure 18B**). Knocking down FOXM1 reduced the mean percentage of EtOH-treated MCF10A-ER-Src cells in S-phase by 1.4-fold. In TAM-treated MCF10A-ER-Src cells, siFOXM1 also reduced the mean percentage of cells in S-phase by 1.3-fold. Yet, these differences were not statistically significant (**Figure 18B**). Noteworthy, amongst the three experimental replicates (represented by different colours in **Figure 18B**), we observed siFOXM1 depletion to be less efficient in one of the replicates (shown in black). In this replicate, in TAM-treated MCF10A-ER-Src cells, siFOXM1 reduced the percentage of cells in S-phase only by 1.5% when compared to cells without siFOXM1 (Mock). Whereas we observed a 7.5% decrease in percentage of TAM-treated cells in S-phase for the other two replicates (shown in red and orange) (**Figure 18B**).

Thus, additional replicate experiments will be required to unequivocally confirm the role of FOXM1 in sustaining cell proliferation in TAM-treated MCF10A-ER-Src cells, although preliminary evidence suggests that FOXM1 might have a role in sustaining the proliferation of TAM-treated cells.

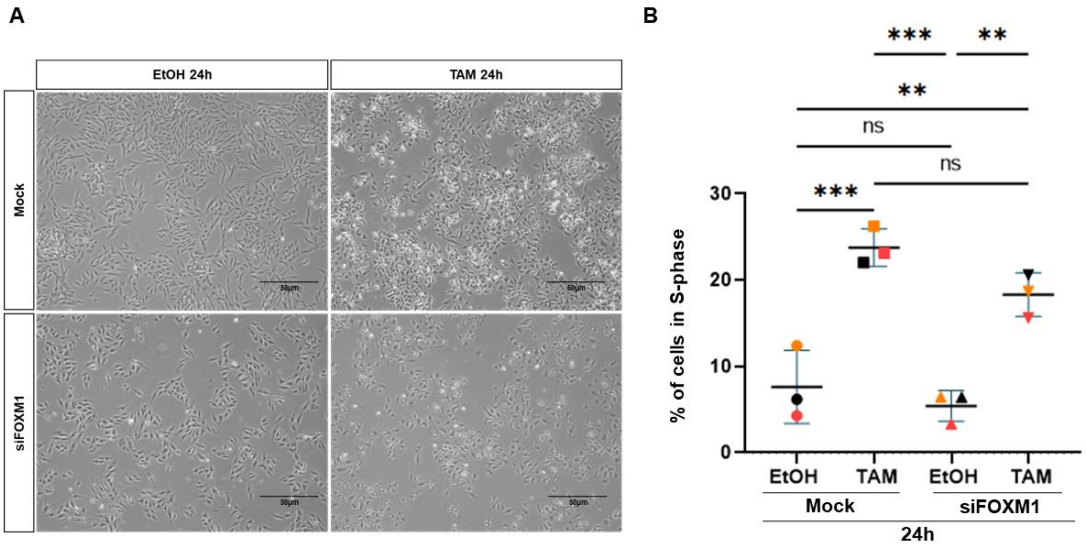

Figure 18. Knocking down FOXM1 appears to reduce the percentage of TAM-treated MCF10A-ER-Src cells in S-phase. (A) Brightfield images of MCF10A-ER-Src cells, transfected without (mock) or with siFOXM1 and treated with EtOH or TAM for 24 hours. Scale bars represent 50µm. **(B**) Percentage (%) from three biological replicates of MCF10A-ER-Src cells in S-phase, transfected without (Mock) or with siFOXM1 and treated with EtOH or TAM for 24 hours. Coloured icons represent distinct experimental replicates. Statistical significance was calculated using one-way ANOVA test. The data are means ± SD. ** *p*-value<0.001, *** *p*-value <0.0001, ns *p*-value >0.05.

CHAPTER V
DISCUSSION

Our findings do not support our starting hypotheses by which an oncogenic form of FOXM1 would be induced in pre-malignant MCF10A-ER-Src cells through the overexpression of specific FOXM1 isoforms (Figure 9). We found that the expression of FOXM1B and FOXM1C is not affected in TAM-treated MCF10A-ER-Src cells during the first 24 hours (Figure 14). Even though we did not analyse the expression levels of FOXM1A or FOXM1D in pre-malignant TAM-treated MCF10A-ER-Src cells, FOXM1A and FOXM1D are unlikely upregulated in these cells, as we found that the anti-FOXM1 N-term and anti-FOXM1 C-term antibodies, which reveal all FOXM1 isoforms, did not show alterations of full length FOXM1 levels (Figure 15 and 16). Thus, these observations suggested that in Src-dependent pre-malignant breast tumours, FOXM1 expression might not be affected. Yet, the original MCF10A cell line was derived from a mastectomy of a pre-menopausal women (Hirsch et al., 2009; Soule et al., 1990). They might therefore remain in a "young" state. Accordingly, while older cells express low FOXM1 levels (Macedo et al., 2018), untransformed MCF10A-ER-Src cells appear to express relatively high levels of FOXM1A, FOXM1B and FOXM1C, alike the colon cancer cell line HCT-116 (Figure 13). Moreover, untransformed MCF10A-ER-Src cells and young fibroblasts show comparable levels of full length FOXM1 by western blot (our data not shown). Therefore, younger cells with high FOXM1 levels might not need to overexpress FOXM1 in order to undergo cellular transformation, which might be the case for older ones. To test this hypothesis, we could test if inducing cellular aging in MCF10A-ER-Src cells by blocking FOXM1 activity using the small molecule inhibitor RCM-1 triggers the upregulation of specific FOXM1 isoforms in pre-malignant cells (L. Sun et al., 2017).

Our findings do not support either the hypotheses by which an oncogenic form of FOXM1 would be induced in pre-malignant MCF10A-ER-Src cells through stabilization or processing of FOXM1 to promote cellular transformation (Figure 9). We observed that full-length FOXM1 is not stabilized during the first 24 hours of TAM treatment in MCF10A-ER-Src cells. Moreover, in these cells, we were unable to provide evidence that TAM treatment triggers the cleavage of full-length FOXM1 (Figure 15 and 16). Therefore, despite previous observations showing that F-actin accumulation stabilizes FOXM1 (Xie et al., 2020) and that ERK might cleave FOXM1C (Lam et al., 2013), our findings suggest that in pre-malignant cells, Src activation does not induce FOXM1 stabilization through F-actin accumulation nor does it cleave FOXM1 by activating ERK. Unexpectedly, we identified a 50kDa form of FOXM1 using an antibody against the N-terminal domain of FOXM1 (Figure 16C). This band should represent a truncated form of FOXM1 since its intensity was decreased in extracts from MCF10A-ER-Src cells (Figure 16A and 16B) and young fibroblasts (our data not shown) transfected with siFOXM1. Nevertheless, Src activation

does not alter the levels of this truncated form during the first 24 hours of TAM treatment in MCF10A-ER-Src cells (Figure 16E). This truncated form of FOXM1, which contains the N-terminal domain, has not been described yet in the literature, but could identify a cleaved FOXM1 form or an additional FOXM1 alternatively spliced isoform.

Instead, our observations support a model by which Src could enhance FOXM1 transcriptional activity, allowing pre-malignant MCF10A-ER-Src cells to sustain proliferation in conditions of restricted serum and growth factor. Consistent with this possibility, our preliminary data suggests that Src activation triggers the transient nuclear translocation of FOXM1 in pre-malignant MCF10A-ER-Src (Figure 17). As a result, FOXM1 might exhibit enhanced transcriptional activity. One mechanism by which Src activation could enhance FOXM1 activity is by phosphorylating FOXM1 directly. In fact, it has been demonstrated that c-Src alleviates the autoinhibition of the TAD by the NRD through phosphorylation (Wierstra, 2011). Alternatively, Src could phosphorylate FOXM1 through ERK activation (Figure 19). Accordingly, activation of the ERK/MAPK pathways can cause FOXM1 to translocate into the nucleus, enhancing FOXM1C's transactivating activity and cell cycle progression through G2/M phase (Ma et al., 2005). Moreover, ERK is required to sustain the proliferation of TAM-treated MCF10A-ER-Src cells (Tavares et al., 2017). Furthermore, constitutively active MEK1 has been shown to enhance the transactivating activity of FOXM1C, but not of FOXM1B (Ma et al., 2005), suggesting that FOXM1C could be the FOXM1 isoform activated by Src in pre-malignant cells. Since Src potentiates ERK activation through F-actin, regulation of the actin cytoskeleton could thus be a critical player in controlling oncogenic FOXM1 in pre-malignant breast cancer cells (Figure 19). Although we were unable to convincingly demonstrate that FOXM1 significantly sustains the proliferation in these cells (Figure 18), an increase in FOXM1 activity could be required for pre-malignant and malignant transformation. Consistent with this hypothesis, FOXM1 is crucial for cell proliferation, and several studies have shown that the down-regulation of FOXM1 expression reduces cell proliferation in breast cancer (C. Yang et al., 2013; M. Wang & Gartel, 2011). However, more experiments are needed to demonstrate that knocking down FOXM1 restricts cell proliferation in pre-malignant MCF10A-ER-Src cells.

Although we could not provide evidence that specific FOXM1 isoforms are upregulated in pre-malignant MCF10A-ER-Src cells (Figure 14), the upregulation of FOXM1 might be required for malignant progression at later stage. Accordingly, RNA sequencing analysis showed that FOXM1 is upregulated in a sub-population of cancer stem-like MCF10A-ER-Src cells treated with TAM for 72 hours (Chang et al., 2015). Moreover, we found through *in silico* ISOexpresso analysis that FOXM1B and FOXM1C could be identified as the two isoforms that are upregulated in Breast carcinoma, Lung Squamous carcinoma, Bladder

Urothelial carcinoma, Colon adenocarcinoma, Lung adenocarcinoma in comparison to normal samples (Figure 11). Hence FOXM1B and FOXM1C could embrace oncogenic functions in malignant cancer cells. Indeed numerous human carcinomas have been demonstrated to have higher levels of FOXM1B and FOXM1C (Halasi & Gartel, 2013). FOXM1B has been shown to have a greater transforming ability than FOXM1C in ovarian cancer cell line and FOXM1B enhances cell migration and invasion in several cancers (Gartel, 2017; Lam et al., 2013; Nakamura et al., 2010). FOXM1C has also been shown to promote cell proliferation, cell migration and invasion in several cancers (Chan et al., 2008; Gartel, 2017; Huang et al., 2014; Zhou et al., 2018). However, we found that prostate adenocarcinoma does not show significant alteration in the expression level of FOXM1A, FOXM1B and FOXM1C. This suggests that these FOXM1 isoforms might not play a crucial role in prostate adenocarcinoma. Additionally, we discovered that FOXM1A was significantly upregulated in Lung Squamous carcinoma but not in any other types of carcinomas we analysed (Figure 11). Most studies conducted to date have focused on FOXM1B and FOXM1C because they are transcriptionally active, which has led to paucity of research on the transcriptionally inactive form FOXM1A, whose function in normal or tumour cells is yet to be determined (Ye et al., 1997). However, it has been proposed that FOXM1A could function as a dominant-negative variant, as it retains normal DNA-binding activity in the absence of a functioning transactivation domain. As a result, FOXM1A could compete with FOXM1B or FOXM1C for binding to FOXM1-binding sites (Laoukili et al., 2007). Hence, it is important to study the effects of knocking down specific FOXM1 isoforms to comprehend their role in triggering cellular transformation.

Interestingly, we also observed that knocking down FOXM1A and FOXM1C in untransformed MCF10A-ER-Src cells transfected with siFOXM1C/A, reduced FOXM1B levels (Figure 13). This observation points to the existence of a mechanism by which FOXM1B expression is maintained by FOXM1C or FOXM1A. As FOXM1 has been shown to activate its own mRNA and protein expression in a positive autoregulatory loop (Halasi & Gartel, 2009). But we cannot fully exclude the possibility that the siFOXM1C/A also knocks down FOXM1B.

Taken together these observations suggest that different FOXM1 isoforms could play different roles in different context during cellular aging and carcinogenesis. FOXM1A could act as tumour suppressor through its dominant negative ability. FOXM1B or FOXM1C could play crucial roles in cellular transformation as oncogenes. In pre-malignant cells, increased activity of FOXM1C could be required to sustain proliferation. FOXM1B has been demonstrated to have most potent transforming ability and FOXM1D has been shown to

promote EMT and metastasis, hence their upregulation could be required for malignant progression.

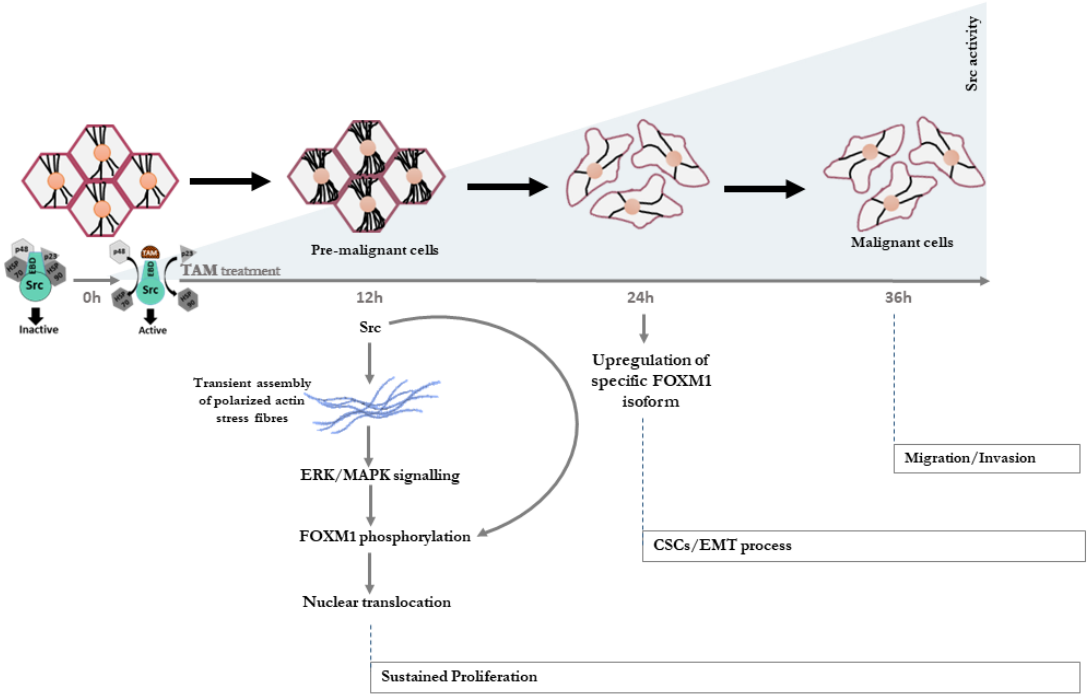

Figure 19. Proposed model by which FOXM1 could be activated by Src to sustain proliferation in MCF10A-ER-Src.

CHAPTER VI
CONCLUSION AND FUTURE PERSPECTIVE

In summary, our observations suggest that an increased in FOXM1 activity could be required to sustain cell proliferation in pre-malignant MCF10A-ER-Src cells. Further experiments are needed to (1) demonstrate that FOXM1 is phosphorylated by Src using Western Blot and kinase assays; (2) to confirm that FOXM1 nuclear re-localization is potentiated in pre-malignant MCF10A-ER-Src cells using IF and Western Blot; (3) to determine if FOXM1 phosphorylation and nuclear translocation involved F-actin by treating cells with Latrunculin A and evaluating the consequences on FOXM1 using IF and Western Blot and (4) to demonstrate that FOXM1 is upregulated in malignant cells by qPCR analysis.

CHAPTER VII
REFERENCES

Abdeljaoued, S., Bettaieb, I., Nasri, M., Adouni, O., Goucha, A., Amine, O. E., Boussen, H., Rahal, K., & Gamoudi, A. (2017). Overexpression of FOXM1 Is a Potential Prognostic Marker in Male Breast Cancer. *Oncology Research and Treatment*, *40*(4), 167–172. https://doi.org/10.1159/000458156

Anders, L., Ke, N., Hydbring, P., Choi, Y. J., Widlund, H. R., Chick, J. M., Zhai, H., Vidal, M., Gygi, S. P., Braun, P., & Sicinski, P. (2011). A Systematic Screen for CDK4/6 Substrates Links FOXM1 Phosphorylation to Senescence Suppression in Cancer Cells. *Cancer Cell*, *20*(5), 620–634. https://doi.org/10.1016/j.ccr.2011.10.001

Aunan, J. R., Cho, W. C., & Søreide, K. (2017). The Biology of Aging and Cancer: A Brief Overview of Shared and Divergent Molecular Hallmarks. *Aging and Disease*, *8*(5), 628–642. https://doi.org/10.14336/AD.2017.0103

Aunan, J. R., Watson, M. M., Hagland, H. R., & Søreide, K. (2016). Molecular and biological hallmarks of ageing. *British Journal of Surgery*, *103*(2), e29–e46. https://doi.org/10.1002/bjs.10053

Bajpai, A., Li, R., & Chen, W. (2021). The cellular mechanobiology of aging: From biology to mechanics. *Annals of the New York Academy of Sciences*, *1491*(1), 3–24. https://doi.org/10.1111/nyas.14529

Berben, L., Floris, G., Wildiers, H., & Hatse, S. (2021). Cancer and Aging: Two Tightly Interconnected Biological Processes. *Cancers*, *13*(6), Article 6. https://doi.org/10.3390/cancers13061400

Bonafè, M., Storci, G., & Franceschi, C. (2012). Inflamm-aging of the stem cell niche: Breast cancer as a paradigmatic example: breakdown of the multi-shell cytokine network fuels cancer in aged people. *BioEssays: News and Reviews in Molecular, Cellular and Developmental Biology*, *34*(1), 40–49. https://doi.org/10.1002/bies.201100104

Castle, J. R., Lin, N., Liu, J., Storniolo, A. M. V., Shendre, A., Hou, L., Horvath, S., Liu, Y., Wang, C., & He, C. (2020). Estimating breast tissue-specific DNA methylation age using next-generation sequencing data. *Clinical Epigenetics*, *12*(1), 45. https://doi.org/10.1186/s13148-020-00834-4

Chan, D., Yu, S., Chiu, P., Yao, K., Liu, V., Cheung, A., & Ngan, H. (2008). Over-expression of FOXM1 transcription factor is associated with cervical cancer progression and pathogenesis. *The Journal of Pathology*, *215*(3), 245–252. https://doi.org/10.1002/path.2355

Chang, C., Goel, H. L., Gao, H., Pursell, B., Shultz, L. D., Greiner, D. L., Ingerpuu, S., Patarroyo, M., Cao, S., Lim, E., Mao, J., McKee, K. K., Yurchenco, P. D., & Mercurio, A. M. (2015). A laminin 511 matrix is regulated by TAZ and functions as the ligand for the α6Bβ1 integrin to sustain breast cancer stem cells. *Genes & Development*, *29*(1), 1–6. https://doi.org/10.1101/gad.253682.114

Egawa, M., Yoshida, Y., Ogura, S., Kurahashi, T., Kizu, T., Furuta, K., Kamada, Y., Chatani, N., Hamano, M., Kiso, S., Hikita, H., Tatsumi, T., Eguchi, H., Nagano, H., Doki, Y., Mori, M., & Takehara, T. (2017). Increased expression of Forkhead box M1 transcription factor is associated with clinicopathological features and confers a poor prognosis in human hepatocellular carcinoma. *Hepatology Research*, *47*(11), 1196–1205. https://doi.org/10.1111/hepr.12854

Fahad Ullah, M. (2019). Breast Cancer: Current Perspectives on the Disease Status. *Advances in Experimental Medicine and Biology*, *1152*, 51–64. https://doi.org/10.1007/978-3-030-20301-6_4

Falandry, C., Bonnefoy, M., Freyer, G., & Gilson, E. (2014). Biology of Cancer and Aging: A Complex Association With Cellular Senescence. *Journal of Clinical Oncology*, *32*(24), 2604–2610. https://doi.org/10.1200/JCO.2014.55.1432

Faria, L., Canato, S., Jesus, T. T., Gonçalves, M., Guerreiro, P. S., Lopes, C. S., Meireles, I., Sá, E. M. de, Paredes, J., & Janody, F. (2022). *Activation of the actin/MRTF-A/SRF signalling pathway in pre-malignant mammary epithelial cells by P-cadherin is essential for transformation* (p. 2022.02.26.481995). bioRxiv. https://doi.org/10.1101/2022.02.26.481995

Feng, Y., Li, S., Zhang, R., Liu, F., Xu, Q., Ding, H., & Teng, Y. (2018). FOXM1 as a prognostic biomarker promotes endometrial cancer progression via transactivation of SLC27A2 expression. *International Journal of Clinical and Experimental Pathology*, *11*(8), 3846–3857.

Field, A. E., Robertson, N. A., Wang, T., Havas, A., Ideker, T., & Adams, P. D. (2018). DNA Methylation Clocks in Aging: Categories, Causes, and Consequences. *Molecular Cell*, *71*(6), 882–895. https://doi.org/10.1016/j.molcel.2018.08.008

Franceschi, C. (2007). Inflammaging as a major characteristic of old people: Can it be prevented or cured? *Nutrition Reviews*, *65*(12 Pt 2), S173-176. https://doi.org/10.1111/j.1753-4887.2007.tb00358.x

Franceschi, C., & Campisi, J. (2014). Chronic Inflammation (Inflammaging) and Its Potential Contribution to Age-Associated Diseases. *The Journals of Gerontology: Series A*, *69*(Suppl_1), S4–S9. https://doi.org/10.1093/gerona/glu057

Figueiredo, J., Rodrigues, I., Ribeiro, J., Fernandes, M. S., Melo, S., Sousa, B., Paredes, J., Seruca, R., & Sanches, J. M. (2018). Geometric compensation applied to image analysis of cell populations with morphological variability: a new role for a classical concept. *Scientific reports*, *8*(1), 10266. https://doi.org/10.1038/s41598-018-28570-z

Gartel, A. L. (2017). FOXM1 in cancer: Interactions and vulnerabilities. *Cancer Research*, *77*(12), 3135–3139. https://doi.org/10.1158/0008-5472.CAN-16-3566

Halasi, M., & Gartel, A. (2009). A novel mode of FoxM1 regulation: Positive auto-regulatory loop. *Cell Cycle (Georgetown, Tex.)*, *8*, 1966–1967. https://doi.org/10.4161/cc.8.12.8708

Halasi, M., & Gartel, A. L. (2013). FOX(M1) news—It is cancer. *Molecular Cancer Therapeutics*, *12*(3), 245–254. https://doi.org/10.1158/1535-7163.MCT-12-0712

Hamurcu, Z., Ashour, A., Kahraman, N., & Ozpolat, B. (2016). FOXM1 regulates expression of eukaryotic elongation factor 2 kinase and promotes proliferation, invasion and tumorgenesis of human triple negative breast cancer cells. *Oncotarget*, *7*(13), 16619–16635. https://doi.org/10.18632/oncotarget.7672

Hanahan, D., & Weinberg, R. A. (2011). Hallmarks of cancer: The next generation. *Cell*, *144*(5), 646–674. https://doi.org/10.1016/j.cell.2011.02.013

Higuchi, R., Vevea, J. D., Swayne, T. C., Chojnowski, R., Hill, V., Boldogh, I. R., & Pon, L. A. (2013). Actin dynamics affects mitochondrial quality control and aging in budding yeast. *Current Biology : CB*, *23*(23), 2417–2422. https://doi.org/10.1016/j.cub.2013.10.022

Higuchi-Sanabria, R., Paul, 3rd, Joseph W., Durieux, J., Benitez, C., Frankino, P. A., Tronnes, S. U., Garcia, G., Daniele, J. R., Monshietehadi, S., & Dillin, A. (2018). Spatial regulation of the actin cytoskeleton by HSF-1 during aging. *Molecular Biology of the Cell*, *29*(21), 2522–2527. https://doi.org/10.1091/mbc.E18-06-0362

Higuchi-Sanabria, R., Vevea, J. D., Charalel, J. K., Sapar, M. L., & Pon, L. A. (2016). The transcriptional repressor Sum1p counteracts Sir2p in regulation of the actin cytoskeleton, mitochondrial quality control and replicative lifespan in Saccharomyces cerevisiae. *Microbial Cell (Graz, Austria)*, *3*(2), 79–88. https://doi.org/10.15698/mic2016.02.478

Hirsch, H. A., Iliopoulos, D., Tsichlis, P. N., & Struhl, K. (2009). Metformin selectively targets cancer stem cells, and acts together with chemotherapy to block tumor growth and prolong remission. *Cancer Research*, *69*(19), 7507–7511. https://doi.org/10.1158/0008-5472.CAN-09-2994

Horvath, S. (2013). DNA methylation age of human tissues and cell types. *Genome Biology*, *14*(10), R115. https://doi.org/10.1186/gb-2013-14-10-r115

Huang, C., Xie, D., Cui, J., Li, Q., Gao, Y., & Xie, K. (2014). FOXM1c Promotes Pancreatic Cancer Epithelial-to-Mesenchymal Transition and Metastasis via Upregulation of Expression of the Urokinase Plasminogen Activator System. *Clinical Cancer Research : An Official Journal of the American Association for Cancer Research*, *20*(6), 1477–1488. https://doi.org/10.1158/1078-0432.CCR-13-2311

Iliopoulos, D., Hirsch, H. A., & Struhl, K. (2009). An Epigenetic Switch Involving NF-κB, Lin28, Let-7 MicroRNA, and IL6 Links Inflammation to Cell Transformation. *Cell*, *139*(4), 693–706. https://doi.org/10.1016/j.cell.2009.10.014

Ito, T., Kohashi, K., Yamada, Y., Iwasaki, T., Maekawa, A., Kuda, M., Hoshina, D., Abe, R., Furue, M., & Oda, Y. (2016). Prognostic Significance of Forkhead Box M1 (FOXM1) Expression and Antitumor Effect of FOXM1 Inhibition in Angiosarcoma. *Journal of Cancer*, *7*(7), 823–830. https://doi.org/10.7150/jca.14461

Ito, T., Kohashi, K., Yamada, Y., Maekawa, A., Kuda, M., Furue, M., & Oda, Y. (2016). Prognostic significance of forkhead box M1 (FoxM1) expression and antitumour effect of FoxM1 inhibition in melanoma. *Histopathology*, *69*(1), 63–71. https://doi.org/10.1111/his.12909

Izdebska, M., Zielińska, W., Hałas-Wiśniewska, M., & Grzanka, A. (2020). Involvement of Actin and Actin-Binding Proteins in Carcinogenesis. *Cells*, *9*(10), 2245. https://doi.org/10.3390/cells9102245

Jain, P. B., Guerreiro, P. S., Canato, S., & Janody, F. (2019). The spectraplakin Dystonin antagonizes YAP activity and suppresses tumourigenesis. *Scientific Reports*, *9*(1), Article 1. https://doi.org/10.1038/s41598-019-56296-z

Johnson, K. S., Conant, E. F., & Soo, M. S. (2021). Molecular Subtypes of Breast Cancer: A Review for Breast Radiologists. *Journal of Breast Imaging*, *3*(1), 12–24. https://doi.org/10.1093/jbi/wbaa110

Kalathil, D., John, S., & Nair, A. S. (2021). FOXM1 and Cancer: Faulty Cellular Signaling Derails Homeostasis. *Frontiers in Oncology*, *10*. https://www.frontiersin.org/articles/10.3389/fonc.2020.626836

Kamińska, M., Ciszewski, T., Łopacka-Szatan, K., Miotła, P., & Starosławska, E. (2015). Breast cancer risk factors. *Przeglad Menopauzalny = Menopause Review*, *14*(3), 196–202. https://doi.org/10.5114/pm.2015.54346

Kaushik, G., Spenlehauer, A., Sessions, A. O., Trujillo, A. S., Fuhrmann, A., Fu, Z., Venkatraman, V., Pohl, D., Tuler, J., Wang, M., Lakatta, E. G., Ocorr, K., Bodmer, R., Bernstein, S. I., Van Eyk, J. E., Cammarato, A., & Engler, A. J. (2015). Vinculin network-mediated cytoskeletal remodeling regulates contractile function in the aging heart. *Science Translational Medicine*, *7*(292), 292ra99. https://doi.org/10.1126/scitranslmed.aaa5843

Khalil, K., Eon, A., & Janody, F. (2022). Cell Architecture-Dependent Constraints: Critical Safeguards to Carcinogenesis. *International Journal of Molecular Sciences*, *23*(15), Article 15. https://doi.org/10.3390/ijms23158622

Knüpfer, H., & Preiss, R. (2007). Significance of interleukin-6 (IL-6) in breast cancer (review). *Breast Cancer Research and Treatment*, *102*(2), 129–135. https://doi.org/10.1007/s10549-006-9328-3

Kong, F.-F., Qu, Z.-Q., Yuan, H.-H., Wang, J.-Y., Zhao, M., Guo, Y.-H., Shi, J., Gong, X.-D., Zhu, Y.-L., Liu, F., Zhang, W.-Y., & Jiang, B. (2014). Overexpression of FOXM1 is associated with EMT and is a predictor of poor prognosis in non-small cell lung cancer. *Oncology Reports*, *31*(6), 2660–2668. https://doi.org/10.3892/or.2014.3129

Kong, X., Li, L., Li, Z., Le, X., Huang, C., Jia, Z., Cui, J., Huang, S., Wang, L., & Xie, K. (2013). Dysregulated Expression of FOXM1 Isoforms Drives Progression of Pancreatic Cancer. *Cancer Research*, *73*(13), 3987–3996. https://doi.org/10.1158/0008-5472.CAN-12-3859

Korver, W., Roose, J., & Clevers, H. (1997). The winged-helix transcription factor Trident is expressed in cycling cells. *Nucleic Acids Research*, *25*(9), 1715–1719.

Korver, W., Roose, J., Heinen, K., Weghuis, D. O., de Bruijn, D., van Kessel, A. G., & Clevers, H. (1997). The human TRIDENT/HFH-11/FKHL16 gene: Structure, localization, and promoter characterization. *Genomics*, *46*(3), 435–442. https://doi.org/10.1006/geno.1997.5065

Kustermans, G., Piette, J., & Legrand-Poels, S. (2008). Actin-targeting natural compounds as tools to study the role of actin cytoskeleton in signal transduction. *Biochemical Pharmacology*, *76*(11), 1310–1322. https://doi.org/10.1016/j.bcp.2008.05.028

Labuhn, M., & Brack, C. (1997). Age-related changes in the mRNA expression of actin isoforms in *Drosophila melanogaster*. *Gerontology*, *43*(5), 261–267. https://doi.org/10.1159/000213861

Laconi, E., Marongiu, F., & DeGregori, J. (2020). Cancer as a disease of old age: Changing mutational and microenvironmental landscapes. *British Journal of Cancer*, *122*(7), Article 7. https://doi.org/10.1038/s41416-019-0721-1

Lai, W.-F., & Wong, W.-T. (2020). Roles of the actin cytoskeleton in aging and age-associated diseases. *Ageing Research Reviews*, *58*, 101021. https://doi.org/10.1016/j.arr.2020.101021

Lam, A. K. Y., Ngan, A. W. L., Leung, M.-H., Kwok, D. C. T., Liu, V. W. S., Chan, D. W., Leung, W. Y., & Yao, K.-M. (2013). FOXM1b, which is present at elevated levels in cancer cells, has a greater transforming potential than FOXM1c. *Frontiers in Oncology*, *3*, 11. https://doi.org/10.3389/fonc.2013.00011

Laoukili, J., Stahl, M., & Medema, R. H. (2007). FoxM1: At the crossroads of ageing and cancer. *Biochimica et Biophysica Acta (BBA) - Reviews on Cancer*, *1775*(1), 92–102. https://doi.org/10.1016/j.bbcan.2006.08.006

Leonardi, G. C., Accardi, G., Monastero, R., Nicoletti, F., & Libra, M. (2018). Ageing: From inflammation to cancer. *Immunity & Ageing : I & A*, *15*, 1. https://doi.org/10.1186/s12979-017-0112-5

Liao, G.-B., Li, X.-Z., Zeng, S., Liu, C., Yang, S.-M., Yang, L., Hu, C.-J., & Bai, J.-Y. (2018). Regulation of the master regulator FOXM1 in cancer. *Cell Communication and Signaling*, *16*(1), 57. https://doi.org/10.1186/s12964-018-0266-6

Limzerwala, J. F., Jeganathan, K. B., Kloeber, J. A., Davies, B. A., Zhang, C., Sturmlechner, I., Zhong, J., Velasco, R. F., Fields, A. P., Yuan, Y., Baker, D. J., Zhou, D., Li, H., Katzmann, D. J., & van Deursen, J. M. (2020). FoxM1 insufficiency hyperactivates

Ect2-RhoA-mDia1 signaling to drive cancer. *Nature Cancer*, *1*(10), 1010–1024. https://doi.org/10.1038/s43018-020-00116-1

Liu, Y., Liu, Y., Yuan, B., Yin, L., Peng, Y., Yu, X., Zhou, W., Gong, Z., Liu, J., He, L., & Li, X. (2017). FOXM1 promotes the progression of prostate cancer by regulating PSA gene transcription. *Oncotarget*, *8*(10), 17027–17037. https://doi.org/10.18632/oncotarget.15224

Livak, K. J., & Schmittgen, T. D. (2001). Analysis of relative gene expression data using real-time quantitative PCR and the 2(-Delta Delta C(T)) Method. *Methods (San Diego, Calif.)*, *25*(4), 402–408. https://doi.org/10.1006/meth.2001.1262

Locke, W. J., Guanzon, D., Ma, C., Liew, Y. J., Duesing, K. R., Fung, K. Y. C., & Ross, J. P. (2019). DNA Methylation Cancer Biomarkers: Translation to the Clinic. *Frontiers in Genetics*, *10*, 1150. https://doi.org/10.3389/fgene.2019.01150

López-Otín, C., Blasco, M. A., Partridge, L., Serrano, M., & Kroemer, G. (2013). The Hallmarks of Aging. *Cell*, *153*(6), 1194–1217. https://doi.org/10.1016/j.cell.2013.05.039

Ly, D. H., Lockhart, D. J., Lerner, R. A., & Schultz, P. G. (2000). Mitotic Misregulation and Human Aging. *Science*, *287*(5462), 2486–2492. https://doi.org/10.1126/science.287.5462.2486

Ma, R. Y. M., Tong, T. H. K., Cheung, A. M. S., Tsang, A. C. C., Leung, W. Y., & Yao, K.-M. (2005). Raf/MEK/MAPK signaling stimulates the nuclear translocation and transactivating activity of FOXM1c. *Journal of Cell Science*, *118*(4), 795–806. https://doi.org/10.1242/jcs.01657

Macedo, J. C., Vaz, S., Bakker, B., Ribeiro, R., Bakker, P. L., Escandell, J. M., Ferreira, M. G., Medema, R., Foijer, F., & Logarinho, E. (2018). FoxM1 repression during human aging leads to mitotic decline and aneuploidy-driven full senescence. *Nature Communications*, *9*(1), Article 1. https://doi.org/10.1038/s41467-018-05258-6

Malhotra, G. K., Zhao, X., Band, H., & Band, V. (2010). Histological, molecular and functional subtypes of breast cancers. *Cancer Biology & Therapy*, *10*(10), 955–960. https://doi.org/10.4161/cbt.10.10.13879

Maslov, A. Y., & Vijg, J. (2009). Genome instability, cancer and aging. *Biochimica et Biophysica Acta*, *1790*(10), 963–969. https://doi.org/10.1016/j.bbagen.2009.03.020

McHugh, D., & Gil, J. (2017). Senescence and aging: Causes, consequences, and therapeutic avenues. *Journal of Cell Biology*, *217*(1), 65–77. https://doi.org/10.1083/jcb.201708092

Medzhitov, R. (2008). Origin and physiological roles of inflammation. *Nature*, *454*(7203), Article 7203. https://doi.org/10.1038/nature07201

Moshier, J. A., Cornell, T., & Majumdar, A. P. N. (1993). Expression of protease genes in the gastric mucosa during aging. *Experimental Gerontology*, *28*(3), 249–258. https://doi.org/10.1016/0531-5565(93)90032-9

Moujaber, O., & Stochaj, U. (2020). The Cytoskeleton as Regulator of Cell Signaling Pathways. *Trends in Biochemical Sciences*, *45*(2), 96–107. https://doi.org/10.1016/j.tibs.2019.11.003

Nakamura, S., Hirano, I., Okinaka, K., Takemura, T., Yokota, D., Ono, T., Shigeno, K., Shibata, K., Fujisawa, S., & Ohnishi, K. (2010). The FOXM1 transcriptional factor promotes the proliferation of leukemia cells through modulation of cell cycle progression in acute myeloid leukemia. *Carcinogenesis*, *31*(11), 2012–2021. https://doi.org/10.1093/carcin/bgq185

Ngan, A. W. L., Grace Tsui, M., So, D. H. F., Leung, W. Y., Chan, D. W., & Yao, K.-M. (2019). Novel Nuclear Partnering Role of EPS8 With FOXM1 in Regulating Cell Proliferation. *Frontiers in Oncology*, *9*, 154. https://doi.org/10.3389/fonc.2019.00154

Okada, K., Fujiwara, Y., Takahashi, T., Nakamura, Y., Takiguchi, S., Nakajima, K., Miyata, H., Yamasaki, M., Kurokawa, Y., Mori, M., & Doki, Y. (2013). Overexpression of Forkhead Box M1 Transcription Factor (FOXM1) is a Potential Prognostic Marker and Enhances Chemoresistance for Docetaxel in Gastric Cancer. *Annals of Surgical Oncology*, *20*(3), 1035–1043. https://doi.org/10.1245/s10434-012-2680-0

Ostan, R., Lanzarini, C., Pini, E., Scurti, M., Vianello, D., Bertarelli, C., Fabbri, C., Izzi, M., Palmas, G., Biondi, F., Martucci, M., Bellavista, E., Salvioli, S., Capri, M., Franceschi, C., & Santoro, A. (2015). Inflammaging and Cancer: A Challenge for the Mediterranean Diet. *Nutrients*, *7*(4), 2589–2621. https://doi.org/10.3390/nu7042589

Panjarian, S., Madzo, J., Keith, K., Slater, C. M., Sapienza, C., Jelinek, J., & Issa, J.-P. J. (2021). Accelerated aging in normal breast tissue of women with breast cancer. *Breast Cancer Research*, *23*(1), 58. https://doi.org/10.1186/s13058-021-01434-7

Pilarsky, C., Wenzig, M., Specht, T., Saeger, H. D., & Grützmann, R. (2004). Identification and validation of commonly overexpressed genes in solid tumors by comparison of microarray data. *Neoplasia (New York, N.Y.)*, *6*(6), 744–750. https://doi.org/10.1593/neo.04277

Provenzano, E., Ulaner, G. A., & Chin, S.-F. (2018). Molecular Classification of Breast Cancer. *PET Clinics*, *13*(3), 325–338. https://doi.org/10.1016/j.cpet.2018.02.004

Ribeiro, R., Macedo, J. C., Costa, M., Ustiyan, V., Shindyapina, A. V., Tyshkovskiy, A., Gomes, R. N., Castro, J. P., Kalin, T. V., Vasques-Nóvoa, F., Nascimento, D. S., Dmitriev, S. E., Gladyshev, V. N., Kalinichenko, V. V., & Logarinho, E. (2022). In vivo cyclic induction of the FOXM1 transcription factor delays natural and progeroid aging phenotypes and extends healthspan. *Nature Aging*, *2*(5), Article 5. https://doi.org/10.1038/s43587-022-00209-9

Sehl, M. E., Henry, J. E., Storniolo, A. M., Ganz, P. A., & Horvath, S. (2017). DNA methylation age is elevated in breast tissue of healthy women. *Breast Cancer Research and Treatment*, *164*(1), 209–219. https://doi.org/10.1007/s10549-017-4218-4

Selvaggio, G., Canato, S., Pawar, A., Monteiro, P. T., Guerreiro, P. S., Brás, M. M., Janody, F., & Chaouiya, C. (2020). Hybrid Epithelial-Mesenchymal Phenotypes Are Controlled by Microenvironmental Factors. *Cancer Research*, *80*(11), 2407–2420. https://doi.org/10.1158/0008-5472.CAN-19-3147

So, K., Tamura, G., Honda, T., Homma, N., Waki, T., Togawa, N., Nishizuka, S., & Motoyama, T. (2006). Multiple tumor suppressor genes are increasingly methylated with age in non-neoplastic gastric epithelia. *Cancer Science*, *97*(11), 1155–1158. https://doi.org/10.1111/j.1349-7006.2006.00302.x

Soule, H. D., Maloney, T. M., Wolman, S. R., Peterson, W. D., Brenz, R., McGrath, C. M., Russo, J., Pauley, R. J., Jones, R. F., & Brooks, S. C. (1990). Isolation and characterization of a spontaneously immortalized human breast epithelial cell line, MCF-10. *Cancer Research*, *50*(18), 6075–6086.

Sun, L., Ren, X., Wang, I.-C., Pradhan, A., Zhang, Y., Flood, H. M., Han, B., Whitsett, J. A., Kalin, T. V., & Kalinichenko, V. V. (2017). The FOXM1 inhibitor RCM-1 suppresses goblet cell metaplasia and prevents IL-13 and STAT6 signaling in allergen-exposed mice. *Science Signaling*, *10*(475), eaai8583. https://doi.org/10.1126/scisignal.aai8583

Sun, Y.-S., Zhao, Z., Yang, Z.-N., Xu, F., Lu, H.-J., Zhu, Z.-Y., Shi, W., Jiang, J., Yao, P.-P., & Zhu, H.-P. (2017). Risk Factors and Preventions of Breast Cancer. *International Journal of Biological Sciences*, *13*(11), 1387–1397. https://doi.org/10.7150/ijbs.21635

Sung, H., Ferlay, J., Siegel, R. L., Laversanne, M., Soerjomataram, I., Jemal, A., & Bray, F. (2021). Global Cancer Statistics 2020: GLOBOCAN Estimates of Incidence and Mortality Worldwide for 36 Cancers in 185 Countries. *CA: A Cancer Journal for Clinicians*, *71*(3), 209–249. https://doi.org/10.3322/caac.21660

Tan, Y., Wang, Q., Xie, Y., Qiao, X., Zhang, S., Wang, Y., Yang, Y., & Zhang, B. (2019). Identification of FOXM1 as a specific marker for triple-negative breast cancer. *International Journal of Oncology*, *54*(1), 87–97. https://doi.org/10.3892/ijo.2018.4598

Tassi, R. A., Todeschini, P., Siegel, E. R., Calza, S., Cappella, P., Ardighieri, L., Cadei, M., Bugatti, M., Romani, C., Bandiera, E., Zanotti, L., Tassone, L., Guarino, D., Santonocito, C., Capoluongo, E. D., Beltrame, L., Erba, E., Marchini, S., D'Incalci, M., … Ravaggi, A. (2017). FOXM1 expression is significantly associated with chemotherapy resistance and adverse prognosis in non-serous epithelial ovarian cancer patients. *Journal of Experimental & Clinical Cancer Research*, *36*(1), 63. https://doi.org/10.1186/s13046-017-0536-y

Tavares, S., Vieira, A. F., Taubenberger, A. V., Araújo, M., Martins, N. P., Brás-Pereira, C., Polónia, A., Herbig, M., Barreto, C., Otto, O., Cardoso, J., Pereira-Leal, J. B., Guck, J., Paredes, J., & Janody, F. (2017). Actin stress fiber organization promotes cell stiffening and proliferation of pre-invasive breast cancer cells. *Nature Communications*, *8*(1), Article 1. https://doi.org/10.1038/ncomms15237

Tchkonia, T., Zhu, Y., Deursen, J. van, Campisi, J., & Kirkland, J. L. (2013). Cellular senescence and the senescent secretory phenotype: Therapeutic opportunities. *The Journal of Clinical Investigation*, *123*(3), 966–972. https://doi.org/10.1172/JCI64098

Teh, M.-T. (2012). FOXM1 coming of age: Time for translation into clinical benefits? *Frontiers in Oncology*, *2*, 146. https://doi.org/10.3389/fonc.2012.00146

Tomasetti, C., & Vogelstein, B. (2015). Variation in cancer risk among tissues can be explained by the number of stem cell divisions. *Science (New York, N.Y.)*, *347*(6217), 78–81. https://doi.org/10.1126/science.1260825

Vasto, S., Candore, G., Balistreri, C. R., Caruso, M., Colonna-Romano, G., Grimaldi, M. P., Listi, F., Nuzzo, D., Lio, D., & Caruso, C. (2007). Inflammatory networks in ageing, age-related diseases and longevity. *Mechanisms of Ageing and Development*, *128*(1), 83–91. https://doi.org/10.1016/j.mad.2006.11.015

Vaz, S., Ferreira, F. J., Macedo, J. C., Leor, G., Ben-David, U., Bessa, J., & Logarinho, E. (2021). FOXM1 repression increases mitotic death upon antimitotic chemotherapy through BMF upregulation. *Cell Death & Disease*, *12*(6), 542. https://doi.org/10.1038/s41419-021-03822-5

Vijg, J., & Suh, Y. (2013). Genome instability and aging. *Annual Review of Physiology*, *75*, 645–668. https://doi.org/10.1146/annurev-physiol-030212-183715

Wang, I.-C., Chen, Y.-J., Hughes, D., Petrovic, V., Major, M. L., Park, H. J., Tan, Y., Ackerson, T., & Costa, R. H. (2005). Forkhead box M1 regulates the transcriptional network of genes essential for mitotic progression and genes encoding the SCF (Skp2-Cks1) ubiquitin ligase. *Molecular and Cellular Biology*, *25*(24), 10875–10894. https://doi.org/10.1128/MCB.25.24.10875-10894.2005

Wang, M., & Gartel, A. L. (2011). The suppression of FOXM1 and its targets in breast cancer xenograft tumors by siRNA. *Oncotarget*, *2*(12), 1218–1226.

Wang, X., Khaidakov, M., Ding, Z., Dai, Y., Mercanti, F., & Mehta, J. L. (2013). LOX-1 in the maintenance of cytoskeleton and proliferation in senescent cardiac fibroblasts. *Journal of Molecular and Cellular Cardiology*, *60*, 184–190. https://doi.org/10.1016/j.yjmcc.2013.04.024

Wang, X., Quail, E., Hung, N.-J., Tan, Y., Ye, H., & Costa, R. H. (2001). Increased levels of forkhead box M1B transcription factor in transgenic mouse hepatocytes prevent age-related proliferation defects in regenerating liver. *Proceedings of the National Academy of Sciences*, *98*(20), 11468–11473. https://doi.org/10.1073/pnas.201360898

Wierstra, I. (2011). The transcription factor FOXM1c is activated by protein kinase CK2, protein kinase A (PKA), c-Src and Raf-1. *Biochemical and Biophysical Research Communications*, *413*(2), 230–235. https://doi.org/10.1016/j.bbrc.2011.08.075

Wierstra, I. (2013). Chapter Six - FOXM1 (Forkhead box M1) in Tumorigenesis: Overexpression in Human Cancer, Implication in Tumorigenesis, Oncogenic Functions, Tumor-Suppressive Properties, and Target of Anticancer Therapy☆☆The present chapter is Part II of a two-part review on the transcription factor FOXM1. Part I of this FOXM1 review is published in Volume 118 of Advances in Cancer Research: Inken Wierstra. The Transcription Factor FOXM1 (Forkhead box M1): Proliferation-Specific Expression, Transcription Factor Function, Target Genes, Mouse Models, and Normal Biological Roles. Advances in Cancer Research, 2013, volume 118, pages 97–398. In K. D. Tew & P. B. Fisher (Eds.), *Advances in Cancer Research* (Vol. 119, pp. 191–419). Academic Press. https://doi.org/10.1016/B978-0-12-407190-2.00016-2

Wierstra, I., & Alves, J. (2007). FOXM1, a typical proliferation-associated transcription factor. *Biological Chemistry*, *388*(12), 1257–1274. https://doi.org/10.1515/BC.2007.159

Witte, T., Plass, C., & Gerhauser, C. (2014). Pan-cancer patterns of DNA methylation. *Genome Medicine*, *6*(8), 66. https://doi.org/10.1186/s13073-014-0066-6

World Health Statistics 2022. (n.d.). Retrieved 13 October 2022, from https://www.who.int/news/item/20-05-2022-world-health-statistics-2022

Wu, Q., Liu, C., Tai, M., Liu, D., Lei, L., Wang, R., Tian, M., & Lü, Y. (2010). Knockdown of FoxM1 by siRNA interference decreases cell proliferation, induces cell cycle arrest and inhibits cell invasion in MHCC-97H cells in vitro. *Acta Pharmacologica Sinica*, *31*(3), Article 3. https://doi.org/10.1038/aps.2010.4

Xie, Z., Janczyk, P. Ł., Zhang, Y., Liu, A., Shi, X., Singh, S., Facemire, L., Kubow, K., Li, Z., Jia, Y., Schafer, D., Mandell, J. W., Abounader, R., & Li, H. (2020). A cytoskeleton regulator AVIL drives tumorigenesis in glioblastoma. *Nature Communications*, *11*(1), Article 1. https://doi.org/10.1038/s41467-020-17279-1

Yang, C., Chen, H., Yu, L., Shan, L., Xie, L., Hu, J., Chen, T., & Tan, Y. (2013). Inhibition of FOXM1 transcription factor suppresses cell proliferation and tumor growth of breast cancer. *Cancer Gene Therapy*, *20*(2), 117–124. https://doi.org/10.1038/cgt.2012.94

Yang, I. S., Son, H., Kim, S., & Kim, S. (2016). ISOexpresso: A web-based platform for isoform-level expression analysis in human cancer. *BMC Genomics*, *17*(1), 631. https://doi.org/10.1186/s12864-016-2852-6

Ye, H., Kelly, T. F., Samadani, U., Lim, L., Rubio, S., Overdier, D. G., Roebuck, K. A., & Costa, R. H. (1997). Hepatocyte nuclear factor 3/fork head homolog 11 is expressed in proliferating epithelial and mesenchymal cells of embryonic and adult tissues. *Molecular and Cellular Biology*, *17*(3), 1626–1641. https://doi.org/10.1128/MCB.17.3.1626

Yin, L., Duan, J.-J., Bian, X.-W., & Yu, S. (2020). Triple-negative breast cancer molecular subtyping and treatment progress. *Breast Cancer Research*, *22*(1), 61. https://doi.org/10.1186/s13058-020-01296-5

Zabransky, D. J., Jaffee, E. M., & Weeraratna, A. T. (2022). Shared genetic and epigenetic changes link aging and cancer. *Trends in Cell Biology*, *32*(4), 338–350. https://doi.org/10.1016/j.tcb.2022.01.004

Zhang, H., Zhong, H., Li, L., Ji, W., & Zhang, X. (2016). Overexpressed transcription factor FOXM1 contributes to the progression of colorectal cancer. *Molecular Medicine Reports*, *13*(3), 2696–2700. https://doi.org/10.3892/mmr.2016.4875

Zhang, X., Pei, Z., Ji, C., Zhang, X., Wang, J. X. and J., Zhang, X., Pei, Z., Ji, C., Zhang, X., & Wang, J. X. and J. (2017). Novel Insights into the Role of the Cytoskeleton in Cancer. In *Cytoskeleton—Structure, Dynamics, Function and Disease*. IntechOpen. https://doi.org/10.5772/66860

Zhang, X., Zhang, L., Du, Y., Zheng, H., Zhang, P., Sun, Y., Wang, Y., Chen, J., Ding, P., Wang, N., Yang, C., Huang, T., Yao, X., Qiao, Q., Gu, H., Cai, G., Cai, S., Zhou, X., & Hu, W. (2017). A novel FOXM1 isoform, FOXM1D, promotes epithelial-mesenchymal transition and metastasis through ROCKs activation in colorectal cancer. *Oncogene*, *36*(6), 807–819. https://doi.org/10.1038/onc.2016.249

Zhao, Z., & Shilatifard, A. (2019). Epigenetic modifications of histones in cancer. *Genome Biology*, *20*(1), 245. https://doi.org/10.1186/s13059-019-1870-5

Zhou, Y., Wang, Q., Chu, L., Dai, W., Zhang, X., Chen, J., Zhang, L., Ding, P., Zhang, X., Gu, H., Zhang, P., Li, L., Zhang, W., Li, L., Lv, X., Zhou, D., Cai, G., Chen, L., Zhao, K., & Hu, W. (2018). FOXM1c promotes oesophageal cancer metastasis by transcriptionally regulating IRF1 expression. *Cell Proliferation*, *52*(2), e12553. https://doi.org/10.1111/cpr.12553

Zinger, A., Cho, W. C., & Ben-Yehuda, A. (2017). Cancer and Aging—The Inflammatory Connection. *Aging and Disease*, *8*(5), 611–627. https://doi.org/10.14336/AD.2016.1230

ANNEX

A

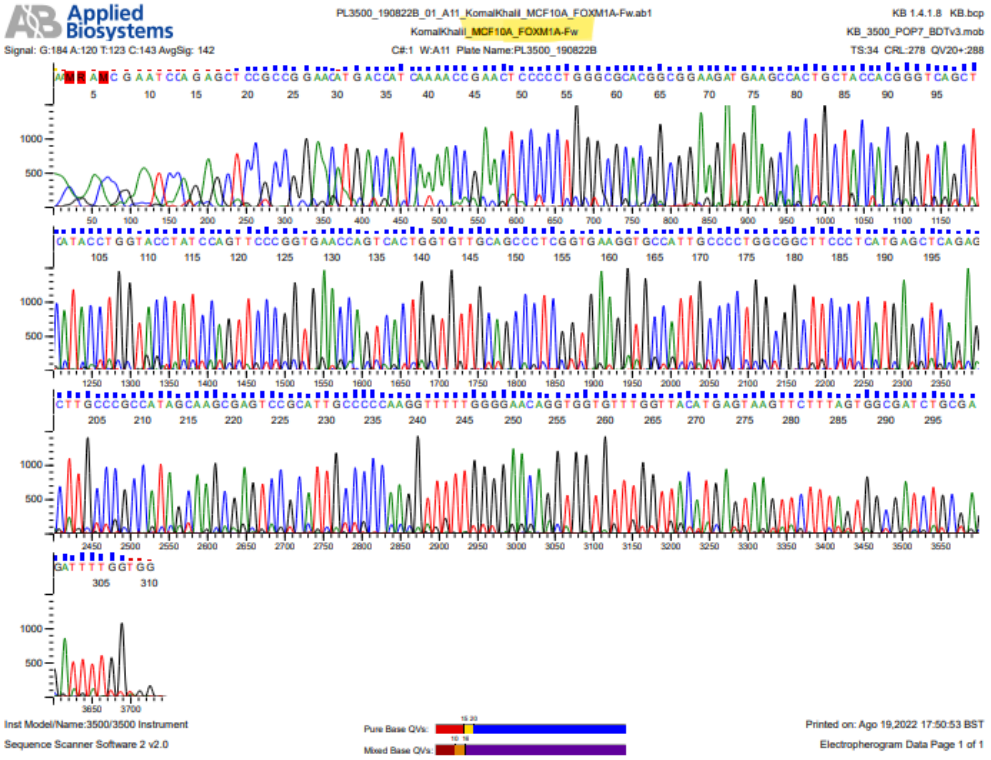
Applied Biosystems
PL3500_190822B_01_A11_KomalKhalil_MCF10A_FOXM1A-Fw.ab1
KomalKhalil_MCF10A_FOXM1A-Fw
C#:1 W:A11 Plate Name:PL3500_190822B
KB 1.4.1.8 KB.bcp
KB_3500_POP7_BDTv3.mob
TS:34 CRL:278 QV20+:288
Signal: G:184 A:120 T:123 C:143 AvgSig: 142
Inst Model/Name:3500/3500 Instrument
Sequence Scanner Software 2 v2.0
Pure Base QVs:
Mixed Base QVs:
Printed on: Ago 19,2022 17:50:53 BST
Electropherogram Data Page 1 of 1

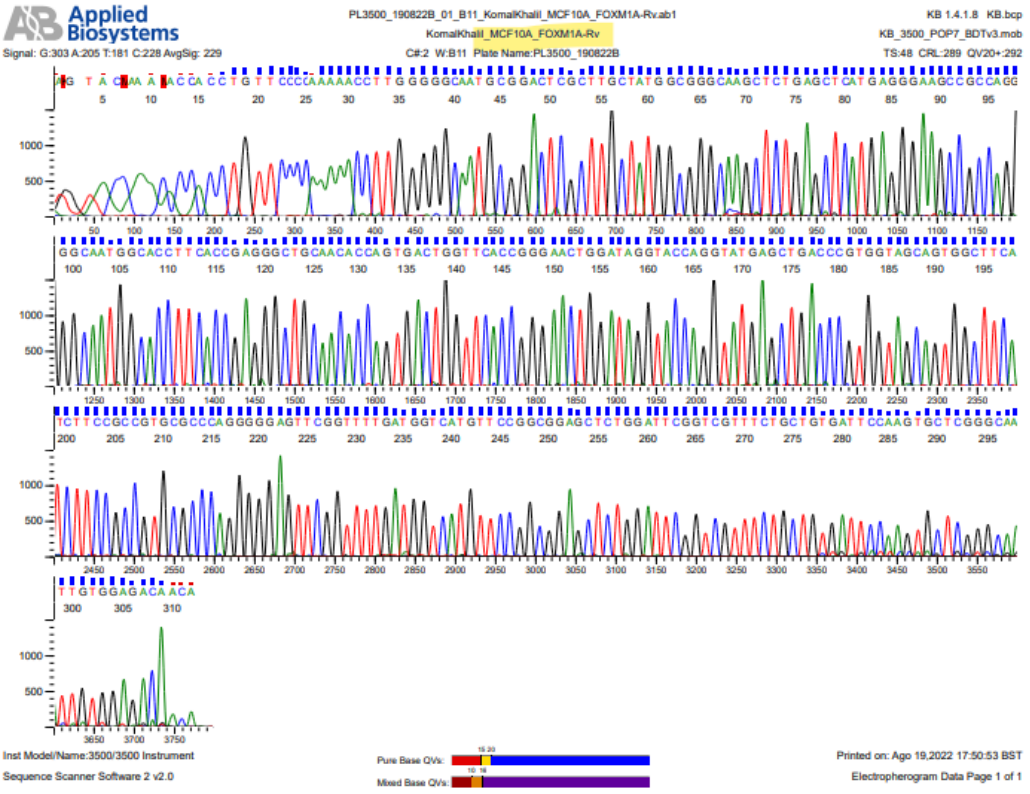
Applied Biosystems
PL3500_190822B_01_B11_KomalKhalil_MCF10A_FOXM1A-Rv.ab1
KomalKhalil_MCF10A_FOXM1A-Rv
C#:2 W:B11 Plate Name:PL3500_190822B
KB 1.4.1.8 KB.bcp
KB_3500_POP7_BDTv3.mob
TS:48 CRL:289 QV20+:292
Signal: G:303 A:205 T:181 C:228 AvgSig: 229
Inst Model/Name:3500/3500 Instrument
Sequence Scanner Software 2 v2.0
Pure Base QVs:
Mixed Base QVs:
Printed on: Ago 19,2022 17:50:53 BST
Electropherogram Data Page 1 of 1

B

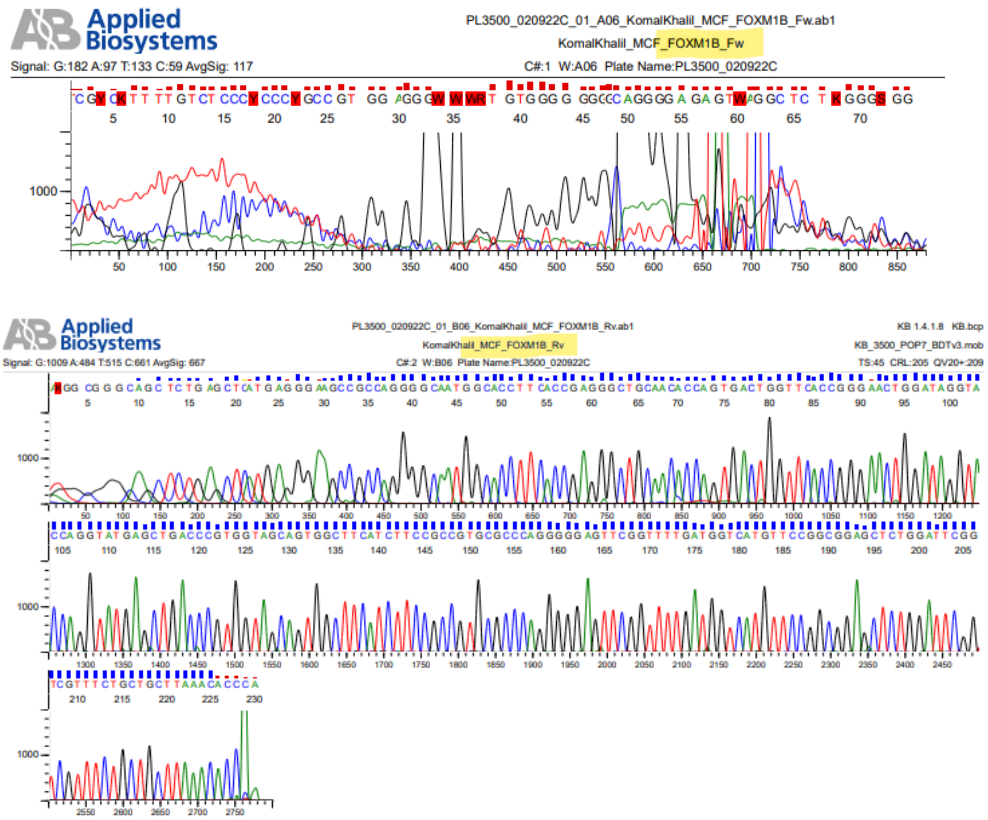

Annex Figure 1. Sanger sequencing data on specific FOXM1 primers. (A) Sanger sequencing data obtained using specific primers for FOXM1A. (B) Sanger sequencing data obtained using specific primers for FOXM1B. FW represents forward primer and RV represents reverse primer.